

A Bidomain Model for Lens Microcirculation

Yi Zhu,¹ Shixin Xu,^{2,*} Robert S. Eisenberg,^{3,4} and Huaxiong Huang^{1,2}

¹Department of Mathematics and Statistics, York University, Toronto, Ontario, Canada; ²Centre for Quantitative Analysis and Modelling, Fields Institute for Research in Mathematical Sciences, Toronto, Ontario, Canada; ³Department of Applied Mathematics, Illinois Institute of Technology, Chicago, Illinois; and ⁴Department of Physiology and Biophysics, Rush University, Chicago, Illinois

ABSTRACT There exists a large body of research on the lens of the mammalian eye over the past several decades. The objective of this work is to provide a link between the most recent computational models and some of the pioneering work in the 1970s and 80s. We introduce a general nonelectroneutral model to study the microcirculation in the lens of the eye. It describes the steady-state relationships among ion fluxes, between water flow and electric field inside cells, and in the narrow extracellular spaces between cells in the lens. Using asymptotic analysis, we derive a simplified model based on physiological data and compare our results with those in the literature. We show that our simplified model can be reduced further to the first-generation models, whereas our full model is consistent with the most recent computational models. In addition, our simplified model captures in its equations the main features of the full computational models. Our results serve as a useful link intermediate between the computational models and the first-generation analytical models. Simplified models of this sort may be particularly helpful as the roles of similar osmotic pumps of microcirculation are examined in other tissues with narrow extracellular spaces, such as cardiac and skeletal muscle, liver, kidney, epithelia in general, and the narrow extracellular spaces of the central nervous system, the “brain.” Simplified models may reveal the general functional plan of these systems before full computational models become feasible and specific.

INTRODUCTION

Biological systems require continual inputs of mass and energy to stay alive. They are open systems that require the flow of matter and specific chemicals across their boundaries. Unicellular organisms can provide that flow by diffusion to and across cell membranes. Diffusion is not adequate over distances larger than a few cell diameters, i.e., larger than 2×10^{-6} m, to pick a number. For that reason, multicellular organisms cannot provide those flows to their cells by diffusion itself. Multicellular organisms depend on convection to bring materials close enough to cells so diffusion to and across cell membranes can provide what the cell needs to live.

The circulatory system of blood vessels—arteries, veins, and capillaries—provides the convection in almost all tissues. But there is one clear exception: the lens of the (mammalian) eye. The lens does not have blood vessels, presumably because even capillaries would seriously interfere with transparency. The lens is large, much larger than the length scale on which diffusion it-

self is efficient. The lens must provide nutrients through another kind of convection, a microcirculation of water that moves nutrients into the lens and rinses wastes out of it. The microcirculation is in fact driven by the lens itself, without an external “pump.” The lens is itself an osmotic pump.

The lens is an asymmetrical electrical syncytium in which all cells are electrically coupled one to another, with a narrow extracellular space between the cells (see Fig. 1). The extracellular space is filled with ionic solution in “free diffusion” with the plasma outside cells. It may also contain specialized, more or less immobile proteins and specialized polysaccharides, as well as containing obstructions formed by the connexin proteins themselves. The intracellular space behaves very much as a large single cell would, with the bioions of classical electrophysiology (Na^+ , K^+ , Cl^-) free to move without much resistance from cell to cell and many solutes of significant size (with a diameter less than 1.5 nm) able to move as well. The intracellular media contains proteins, particularly the crystallins responsible for the high refractive index of the lens. So, the lens is an example of a bidomain tissue that has been studied in some detail, first in skeletal muscle, then in cardiac muscle and syncytia in general. Electrical models of bidomain tissues have been developed, and a general approach combining morphology,

Submitted December 3, 2018, and accepted for publication February 13, 2019.

*Correspondence: sxu@fields.utoronto.ca

Editor: Brian Salzberg.

<https://doi.org/10.1016/j.bpj.2019.02.007>

© 2019 Biophysical Society.



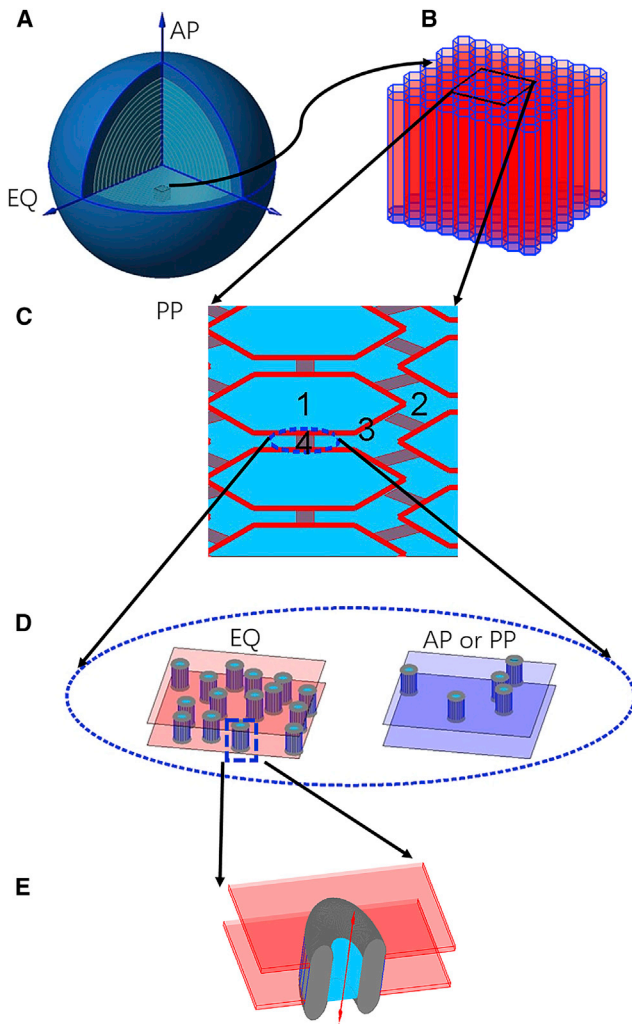


FIGURE 1 Schematic diagram of lens. (A) The sphere of the lens is shown with three landmarks: anterior pole (AP), posterior pole (PP), and equator (EQ). (B) The control volume in the bidomain model is shown. (C) The microstructure of the lens is shown: 1) intracellular region, 2) extracellular region, 3) cell membrane, and 4) gap junction (connections). (D) Distribution of the gap junctions between the cell membrane at EQ or AP and PP are shown. (E) A single gap junction that allows the water and ion flows is shown. To see this figure in color, go online.

theory, and experiments has been applied in (1), showing how the lens could be studied in this tradition.

A general approach to bidomain tissues was implemented (2) involving detailed measurements of morphology (best done with statistical sampling by stereological methods (3)), impedance spectroscopy (4–10) using intracellular probes (microelectrodes) that force current to flow across membranes to the extracellular baths (1,11–15), electric field theory to develop models appropriate to the structure (16–20), analyzing the spectroscopic data with the field theory (21,22), and checking that parameters change appropriately (i.e., estimates of membrane capacitance are constant) as extracellular solutions are changed in composition and concentration (20,23). This work was extended to deal

with transport by Mathias and co-workers (24–40), and computational models of the water flow in the lens were later developed in some detail (25,41,42) and exploited with great success (reviewed in (43,44); also see (45–49)).

The original work on electrical models is cited here because it provides coherent support, involving a range of techniques and approaches, to the general view of syncytial tissues used here and in later work. It also shows the range of approaches needed to establish a (then) new view of a tissue.

Mathias (50,51) realized that an asymmetrical electrical syncytium would produce convection, in particular in the lens (31); he and co-workers systematically investigated the flow of water, solutes, and current in the lens, and their work is (in our opinion) a model of interdisciplinary research, combining theory, simulation, and measurements of many types (24–40). Computational models of the water flow in the lens were later developed in great detail (25,41,42) and compared to the more analytical models. These models have been extensively tested, and we are fortunate that comprehensive reviews have been written of great value to newcomers to the field, particularly (43,44) as well as (41,43–49).

Since the pioneering work on the models of lens microcirculation system proposed by Mathias et al. (21,51), numerous investigations have been carried out (19,20,23,52,53). The microcirculation model has firstly relied on a combination of electrical resistance and current measurements and theoretical modeling (18,19,54). More recently, to provide a better understanding of the electric current flow and potential field, the detailed structure of lens has been included (41,43–55), describing the asymmetric biological properties of the lens, and measurements of pressure have been made (28,47). Different types of fluid flow (56,57) and transport properties of the ions have been introduced. Meanwhile, the lens model (55) has been extended to simulate age-related changes in lens physiology (58) and a variety of physiological processes (26,59–61). Reviews of current studies on microcirculation in lens are most helpful (26,30,33). Despite this large body of experimental and theoretical work, it is not completely clear how they are related to each other. In particular, it is not clear how the latest computational models are related to the pioneering work and how theoretical analysis is related to experimental findings. In this work, we will provide such a link.

Based on the microscale model for semipermeable membranes (62) and the bidomain method (51), we construct a mathematical model to ensure that all interactions are included and treated consistently. Using asymptotic analysis, we derive a reduced model, which can be used to obtain most physiologically significant quantities except for the intracellular pressure. This simplified model can be further reduced to the model proposed by Mathias (51) with additional assumptions that Nernst potentials (which describe gradients of chemical potential of each ionic species) and

conductance are constant in space. However, we will show that neither the Nernst potentials nor the conductance are constant. On the contrary, they vary significantly from the interior to the surface of the lens. Therefore, both of these quantities need to be coupled as part of the solution.

Our model also shows explicitly that the intracellular pressure is decoupled from the rest of the variables. Evolution has chosen parameters, so the intracellular pressure does not affect the other parameters of the lens in a significant way. They are robust to variations of intracellular pressure. The evolutionary advantage of this adaptation is not clear to us but may be more obvious to other workers with a greater knowledge of clinical realities that show how the lens becomes diseased (46,48,49,63). Our simplified model suggests that all the quantities can be computed without knowing the intracellular pressure. On the other hand, we need to solve the full model to find the value of the intracellular pressure. Our model is also calibrated by experimental data and predicts the effects of gap junctions (28,47) described by a “membrane” permeability κ_{in} .

Our new results extend but do not fundamentally change previous work on the lens. We strengthen the view that the lens provides an osmotic pump to maintain the microcirculation necessary to sustain a living lens for the life of the animal. We imagine that similar osmotic pumps create microcirculation in other cells and tissues of the body.

This study is organized as follows. The full model for microcirculation of water and ions are proposed based on conservation laws in [Mathematical Model](#). In [Simplified Model](#), we obtain the leading-order model by identifying small parameters in the full model. Based on the boundary conditions and partial differential equation analysis, a simplified version of the leading-order model is proposed and compared with the existing models. The model calibration and simulation results are shown in [Results and Discussion](#). The conclusions and future work are given in [Conclusions](#).

METHODS

Mathematical model

In this section, we present a one-dimensional spherical symmetric nonelectroneutral model for microcirculation of the lens with radius R by using the bidomain method (17). The model deals with two types of flow: the circulation of water (hydrodynamics) and the circulation of ions (electrodynamics), generalizing previous bidomain models that deal only with electrodynamics. The model is mainly derived from laws of conservation of ions and water in the presence of membrane flow between intra- and extracellular domains. We note that a similar approach may be useful in other tissues with narrow extracellular space, such as the heart, cardiac muscle, and the central nervous system, including the cerebral cortex, the “brain.”

Water circulation

We assume the following:

1. the loss of intracellular water is only through membranes flowing into the extracellular space and vice versa (17);

2. the transmembrane water flux is proportional to the intra/extracellular hydrostatic pressure and osmotic pressure differences (i.e., Starling’s law, classically applied to capillaries, here applied to membranes (64)). In a system like nonideal ionic solutions in which “everything interacts with everything else” (65,66), this statement needs derivation as well as assertion. A complete and rigorous derivation can be found in (62);
3. in the rest of this work, the subscript $l = in, ex$ denotes the intra/extracellular space and superscript $i = Na^+, K^+, Cl^-$ denotes the i th species ion.

Then, we obtain the following system for intra- and extracellular velocities in domain $\Omega = [0, R]$:

$$\begin{aligned} & \frac{1}{r^2} \frac{d}{dr} (r^2 \mathcal{M}_{ex} u_{ex}) \\ & = -\mathcal{M}_v L_m (P_{ex} - P_{in} + \gamma_m k_B T (O_{in} - O_{ex})) \end{aligned} \quad (1a)$$

and

$$\frac{1}{r^2} \frac{d}{dr} (r^2 (\mathcal{M}_{ex} u_{ex} + \mathcal{M}_{in} u_{in})) = 0, \quad (1b)$$

where u_l and P_l are the velocity and pressure in the intracellular and extracellular space, respectively, and O_l is the osmotic pressure with definition

$$O_{ex} = \sum_i C_{ex}^i, \quad O_{in} = \sum_i C_{in}^i + \frac{A_{in}}{V_{in}},$$

where C_l^i is the concentration of i th species ion in l space and A_{in}/V_{in} is the density of the permanent negatively charged protein. In this work, we assume the permanent negative charged protein is uniformly distributed within intracellular space with a valence of \bar{z} . Here, \mathcal{M}_l is the ratio of intracellular area ($l = in$) and extracellular area ($l = ex$), \mathcal{M}_v is the membrane area per volume unit, γ_m is the intracellular membrane reflectance, L_m is intracellular membrane hydraulic permeability, k_B is the Boltzmann constant, and T is temperature.

As we mentioned before, the intracellular space is a connected space, where water can flow from cell to cell through connexin proteins joining membranes of neighboring cells, and the extracellular space is narrow, with a high tortuosity. The intracellular velocity depends on the gradients of hydrostatic pressure and osmotic pressure (41,51,62), and the extracellular velocity is determined by the gradients of hydrostatic pressure and electric potential (41,67),

$$u_{ex} = -\frac{\kappa_{ex}}{\mu} \tau_c \frac{d}{dr} P_{ex} - k_e \tau_c \frac{d}{dr} \phi_{ex} \quad (2a)$$

and

$$u_{in} = -\frac{\kappa_{in}}{\mu} \left(\frac{d}{dr} P_{in} - \gamma_m k_B T \frac{d}{dr} O_{in} \right), \quad (2b)$$

where ϕ_l is the electric potential in the l space, τ_c is the tortuosity of extracellular region, μ is the viscosity of water, k_e is introduced to describe the effect of electro-osmotic flow, and κ_l is the permeability of the intracellular region ($l = in$) and the extracellular region ($l = ex$), respectively.

Thanks to Eq. 2, Eq. 1 can be treated as an equation of hydraulic pressure. Because of the axis symmetry condition, homogeneous Neumann boundary conditions are used for pressure at $r = 0$. At the surface of lens $r = R$, we set the extracellular hydrostatic pressure to be zero, and the intracellular velocity is consistent with Eq. 2

$$\begin{cases} \frac{\partial P_{ex}}{\partial r} = \frac{\partial P_{in}}{\partial r} = 0, & \text{at } r = 0, \\ P_{ex} = 0, & \text{at } r = R, \\ -\frac{\kappa_{in}}{\mu} \left(\frac{d}{dr} P_{in} - \gamma_m k_B T \frac{d}{dr} O_{in} \right) \\ = L_s (P_{in} - \gamma_s k_B T (O_{in} - O_{ex})), & \text{at } r = R, \end{cases} \quad (3)$$

where γ_s is surface membrane reflectance and L_s is surface membrane hydraulic permeability.

Ion circulation

With similar assumptions, the conservation of ion concentration yields the following ion flux system:

$$\frac{1}{r^2} \frac{d}{dr} (r^2 \mathcal{M}_{ex} J_{ex}^i) = \mathcal{M}_v J_m^i \quad (4a)$$

and

$$\frac{1}{r^2} \frac{d}{dr} (r^2 (\mathcal{M}_{ex} J_{ex}^i + \mathcal{M}_{in} J_{in}^i)) = 0. \quad (4b)$$

The ion flux in the intracellular region J_{in}^i and ion flux in the extracellular region J_{ex}^i are defined as

$$J_{ex}^i = C_{ex}^i u_{ex} - D_{ex}^i \tau_c \frac{d}{dr} C_{ex}^i - D_{ex}^i \tau_c \frac{z^i e}{k_B T} C_{ex}^i \frac{d}{dr} \phi_{ex}, \quad (5a)$$

$$J_{in}^i = C_{in}^i u_{in} - D_{in}^i \frac{d}{dr} C_{in}^i - D_{in}^i \frac{z^i e}{k_B T} C_{in}^i \frac{d}{dr} \phi_{in}, \quad (5b)$$

where D_l^i is the diffusion coefficient of the i th species ion in the l space. The intracellular medium can be well described by a single diffusion coefficient despite it being crowded with solute: current and ions move around the solutes, rather like water flowing around a ship, changing the effective diffusion coefficient and little else, as they do in skeletal muscle (68,69), where the cytoplasm (i.e., myoplasm) is even more crowded with ions and structures than the lens.

The Ohm's law conductance formulation is used to describe the transmembrane flux of ions across intracellular membrane and surface membrane

$$j_m^i = \frac{g^i}{e z^i} (\phi_{in} - \phi_{ex} - E^i), \quad (6a)$$

$$j_s^i = \frac{G^i}{e z^i} (\phi_{in} - \phi_{ex} - E^i), \quad (6b)$$

where $E^i = k_B T / e z^i \log(C_{ex}^i / C_{in}^i)$ is the Nernst potential (an expression of the difference of chemical potential) of the i th species ion.

In Eq. 6, the intracellular ion conductance g^i and surface ion conductance G^i depends on the ion channel distribution on the membrane (see Fig. 2). Based on previous work (17,41,51), we assume that 1) only Na^+ and Cl^- can leak between intracellular and extracellular through ion channels inside the lens and 2) there is no transmembrane flux for K^+ between the extracellular and intracellular region, i.e., $j_m^K = 0$.

Similarly, homogeneous Neumann boundary conditions are used at $r = 0$. At $r = R$, the extracellular concentrations are fixed, and Robin boundary

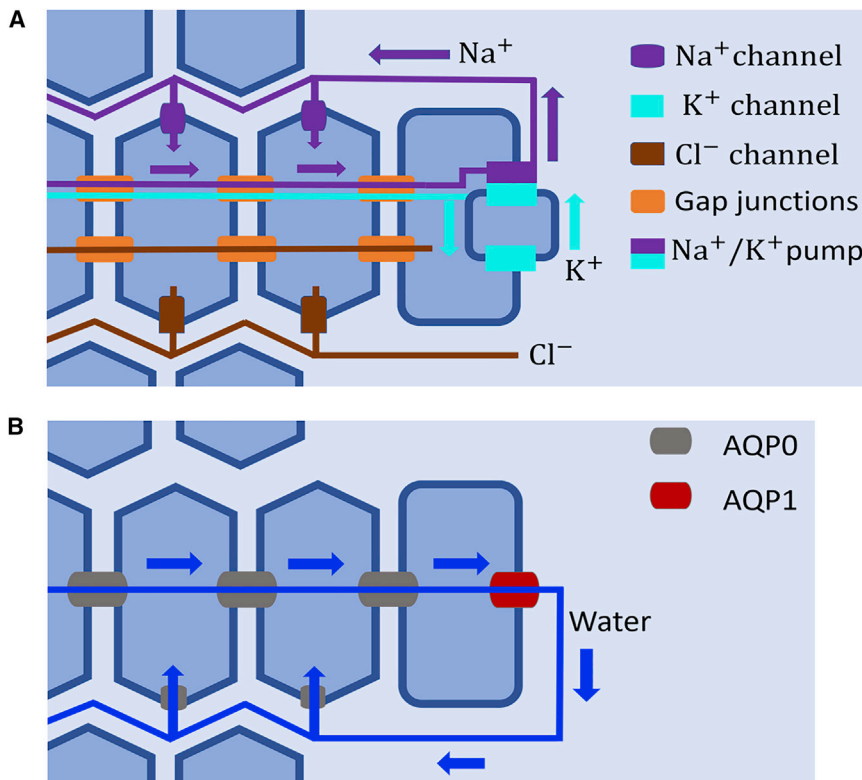


FIGURE 2 (A) Schematic diagram of ion circulation and the distributions of ion channels and pumps. The purple line represents the sodium circulation, the light green represents the potassium circulation, and the brown line represents chloride circulation. The surface epithelial cells (dark blue square) connect with the intracellular cells (light blue hexagon) by the gap junctions (orange rectangle). The sodium and chlorine ion channels are located on the intracellular membranes, whereas the potassium ion channel and sodium-potassium ATP pumps are found only on the surface membrane. (B) A schematic diagram of water circulation is shown. Transmembrane water transport is through AQP0 and AQP1 gap junctions. AQP0 gap junctions are located on the intracellular membranes, and AQP1 is on the surface membrane. To see this figure in color, go online.

conditions are used for intracellular concentrations because of the transmembrane flux and pump:

$$\begin{cases} J_{ex}^i = J_{in}^i = 0, & \text{at } r = 0 \\ C_{ex}^i = C_o^i, J_{in}^i = j_s^i + a^i, & \text{at } r = R, \end{cases} \quad (7)$$

where a^i is an active ion pump on the surface membrane. Here, we only consider the sodium-potassium pump on the surface. The strength of the pump depends on the ion's concentration as in (29,41),

$$a^{Na} = 3\frac{I_p}{e}, \quad a^K = -2\frac{I_p}{e}, \quad a^{Cl} = 0, \quad (8)$$

where

$$\begin{aligned} I_p = I_{max1} & \left(\frac{C_{in}^{Na}}{C_{in}^{Na} + K_{Na1}} \right)^3 \left(\frac{C_o^K}{C_o^K + K_{K1}} \right)^2 \\ & + I_{max2} \left(\frac{C_{in}^{Na}}{C_{in}^{Na} + K_{Na2}} \right)^3 \left(\frac{C_o^K}{C_o^K + K_{K2}} \right)^2. \end{aligned} \quad (9)$$

Because of the capacitance of the cell membrane, assumptions of exact charge neutrality can easily lead to paradoxes because they oversimplify Maxwell's equations by leaving out altogether the essential role of charge. We use the analysis of (70) and thus introduce a linear correction term replacing the charge neutrality condition (41,51) without introducing significant error (see also (71)),

$$(1 - \eta) \left(\sum_i e z^i C_{ex}^i \right) = -\mathcal{M}_v C_m (\phi_{in} - \phi_{ex}) \quad (10a)$$

and

$$\eta \left(\sum_i e z^i C_{in}^i + \bar{z} e \frac{A_{in}}{V_{in}} \right) = \mathcal{M}_v C_m (\phi_{in} - \phi_{ex}), \quad (10b)$$

where η is the porosity of intracellular region and C_m is capacitance per unit area.

Multiplying each ion concentration equation in Eq. 4 with $e z^i$, respectively, summing up, and using Eq. 10, the sodium equations are replaced by the following equations:

$$\begin{aligned} & \frac{1}{r^2} \frac{d}{dr} \left(r^2 \mathcal{M}_{ex} \left(\rho_{ex} u_{ex} - e \tau_c \sum_i D_{ex}^i z^i \frac{d}{dr} C_{ex}^i - \sigma_{ex} \frac{d}{dr} \phi_{ex} \right) \right) \\ & = \mathcal{M}_v \left(g^m (\phi_{in} - \phi_{ex}) - \sum_i g^i E^i \right) \end{aligned} \quad (11a)$$

$$\begin{aligned} & \frac{1}{r^2} \frac{d}{dr} \left(r^2 \mathcal{M}_{in} \left(\rho_{in} u_{in} - e \sum_i D_{in}^i z^i \frac{d}{dr} C_{in}^i - \sigma_{in} \frac{d}{dr} \phi_{in} \right) \right) \\ & = -\mathcal{M}_v \left(g^m (\phi_{in} - \phi_{ex}) - \sum_i g^i E^i \right) \end{aligned} \quad (11b)$$

with boundary conditions

$$\begin{cases} \frac{d\phi_{ex}}{dr} = \frac{d\phi_{in}}{dr} = 0, & \text{at } r = 0, \\ \phi_{ex} = 0, & \text{at } r = R, \\ \left(\rho_{in} u_{in} - e \sum_i D_{in}^i z^i \frac{d}{dr} C_{in}^i - \sigma_{in} \frac{d}{dr} \phi_{in} \right) \\ = G^s \phi_{in} - \sum_i G^i E^i + I_p^\phi, & \text{at } r = R, \end{cases}$$

where $\rho_{in} = \mathcal{M}_v C_m / \eta (\phi_{in} - \phi_{ex}) + |\bar{z}| e A_{in} / V_{in}$ and $\rho_{ex} = \mathcal{M}_v C_m / (1 - \eta) (\phi_{ex} - \phi_{in})$

$$g^m = \sum_i g^i, \quad G^s = \sum_i G^i, \quad I_p^\phi = e \sum_i z^i a^i.$$

In Eq. 11, we define the intracellular conductance σ_{in} and extracellular conductance σ_{ex} as

$$\begin{aligned} \sigma_{ex} & = \frac{e^2 \tau_c}{k_B T} \left(\sum_i D_{ex}^i (z^i)^2 C_{ex}^i \right), \\ \sigma_{in} & = \frac{e^2}{k_B T} \left(\sum_i D_{in}^i (z^i)^2 C_{in}^i \right). \end{aligned}$$

It is obvious that system 11 might be derived using either Eqs. 4 or 10. Therefore, we should drop either Eqs. 4 or 10 when Eq. 11 is used.

Nondimensionalization

Because lens circulation is driven by the sodium-potassium pump, it is natural to choose the characteristic velocity u_{in}^* by the pump strength a^{Na*} :

$$u_{in}^* = \frac{a^{Na*}}{O^*}, \quad (12)$$

where $O^* = 2(C_o^{Na} + C_o^K)$ is characteristic osmotic pressure. Using Eq. 1b, we obtain the scale of u_{ex} as

$$u_{ex}^* = \delta_0^{-1} u_{in}^*, \quad (13)$$

where $\delta_0 = \mathcal{M}_{ex} / \mathcal{M}_{in}$. With the characteristic values for ϕ , P , C^i , chosen as $k_B T / e$, $\mu R u_{ex}^* / \kappa_{ex} \tau_c$, and $C_o^{Na} + C_o^K$, we obtain the dimensionless system for lens problem as follows (a detailed derivation is given in Appendix C in the Supporting Materials and Methods):

$$u_{ex} = -\frac{d}{dr} P_{ex} - \delta_1 \frac{d}{dr} \phi_{ex}, \quad (14a)$$

$$\delta_2 u_{in} = -\delta_3 \frac{d}{dr} P_{in} + \frac{d}{dr} O_{in}, \quad (14b)$$

$$\delta_4 \frac{1}{r^2} \frac{d}{dr} (r^2 u_{in}) = \delta_3 (P_{ex} - P_{in}) + (O_{in} - O_{ex}), \quad (14c)$$

$$u_{ex} = -u_{in}, \quad (14d)$$

$$\sum_i z^i C_{in}^i + \frac{\bar{z} A_{in}}{V_{in}} = \delta_6 (\phi_{in} - \phi_{ex}), \quad (14e)$$

$$\sum_i z^i C_{ex}^i = -\delta_7(\phi_{in} - \phi_{ex}), \quad (14f)$$

$$\frac{1}{r^2} \frac{d}{dr} (r^2 J_{ex}^{Cl}) = \frac{\mathcal{M}_v^{ex}}{z^{Cl}} (\phi_{in} - \phi_{ex} - E^{Cl}), \quad (14g)$$

$$\frac{1}{r^2} \frac{d}{dr} (r^2 J_{in}^{Cl}) = -\frac{\delta_8}{r^2} \frac{d}{dr} (r^2 J_{ex}^{Cl}), \quad (14h)$$

$$\frac{1}{r^2} \frac{d}{dr} (r^2 J_{ex}^K) = 0, \quad (14i)$$

$$\frac{1}{r^2} \frac{d}{dr} (r^2 J_{in}^K) = 0, \quad (14j)$$

$$\begin{aligned} & \frac{1}{r^2} \frac{d}{dr} \left(r^2 \left(P e_{ex} \rho_{ex} u_{ex} - \sum_i D_{ex}^i z^i \frac{d}{dr} C_{ex}^i - \sigma_{ex} \frac{d}{dr} \phi_{ex} \right) \right), \\ & = \mathcal{M}_v^{ex} (2(\phi_{in} - \phi_{ex}) - E^{Na} - E^{Cl}) \end{aligned} \quad (14k)$$

$$\begin{aligned} & \frac{1}{r^2} \frac{d}{dr} \left(r^2 \left(P e_{in} \rho_{in} u_{in} - \sum_i D_{in}^i z^i \frac{d}{dr} C_{in}^i - \sigma_{in} \frac{d}{dr} \phi_{in} \right) \right) \\ & = -\frac{\delta_8}{r^2} \frac{d}{dr} \left(r^2 \left(P e_{ex} \rho_{ex} u_{ex} - \sum_i D_{ex}^i z^i \frac{d}{dr} C_{ex}^i - \sigma_{ex} \frac{d}{dr} \phi_{ex} \right) \right), \end{aligned} \quad (14l)$$

with homogeneous Neumann boundary conditions at $r = 0$ and the following boundary conditions at $r = 1$:

$$\left\{ \begin{array}{l} P_{ex} = 0, \\ \delta_5 u_{in} = \delta_3 P_{in} - (O_{in} - O_{ex}), \\ C_{ex}^K = C_o^K, \quad J_{in}^K = \frac{R_s}{z_K} (\phi_{in} - E^K) - a^K, \\ C_{ex}^{Cl} = \tilde{C}_o^{Na} + \tilde{C}_o^K + \delta_7 (\tilde{\phi}_{in} - \tilde{\phi}_{ex}), \quad J_{in}^{Cl} = 0, \\ \phi_{ex} = 0, \\ P e_{in} \rho_{in} u_{in} - \sum_i D_{in}^i z^i \frac{d}{dr} C_{in}^i - \sigma_{in} \frac{d}{dr} \phi_{in} \\ = \frac{R_s}{z_K} (\phi_{in} - E^K) + I_p^\phi, \end{array} \right.$$

where

$$\rho_{in} = \rho_0 + \delta_6 (\phi_{in} - \phi_{ex}), \quad \rho_0 = |\bar{z}| \frac{A_{in}}{V_{in}}, \quad (15a)$$

$$\rho_{ex} = \delta_7 (\phi_{ex} - \phi_{in}), \quad (15b)$$

$$\sigma_l = \sum_i D_l^i (z^i)^2 C_l^i, \quad (15c)$$

$$E^i = \frac{1}{z^i} \log \left(\frac{C_{ex}^i}{C_{in}^i} \right), \quad (15d)$$

$$I_p^\phi = \frac{I_p R}{e D_{in}^* C^*}, \quad (15e)$$

and

$$J_l^i = P e_l C_l^i u_l - D_l^i \left(\frac{d}{dr} C_l^i + z^i C_l^i \frac{d}{dr} \phi_l \right). \quad (15f)$$

Simplified model

The full model given by system 14 with boundary condition 15 is a coupled nonlinear system. In this section, we present a simplified version of the full model that captures the main features of the lens circulation. We first obtain the leading-order model by identifying the small parameters. Then, by using boundary conditions and theoretical analysis, the leading-order model is further simplified as only one partial differential equation with serial algebra equations.

According to those dimensionless parameters presented in Appendix B in the [Supporting Materials and Methods](#), we identify the scale of the parameters as follows:

$$\begin{aligned} \{\delta_1, \delta_8\} &\subset O(\epsilon), \quad \{\delta_0, \delta_3\} \subset O(\epsilon^2), \\ \{\delta_2, \delta_4, \delta_5, \delta_6, \delta_7\} &\subset o(\epsilon^2). \end{aligned} \quad (16)$$

If we denote $\delta_9 = D_l^{Cl} - D_l^K$ and $\delta_{10} = D_l^{Cl} - D_l^{Na}$, $l = in, ex$, it yields

$$\delta_9 = O(\epsilon^2), \quad \delta_{10} = O(\epsilon). \quad (17)$$

A priori estimation

In this section, we provide the priori estimation of the J_{in}^{Cl} as follows. By using the homogeneous Neumann boundary condition at $r = 0$, Eq. 14l yields

$$\begin{aligned} \frac{d}{dr} \phi_{in} &= \frac{1}{\sigma_{in}} \left(P e_{in} \rho_{in} u_{in} + \delta_9 \frac{d}{dr} C_{in}^K + \delta_{10} \frac{d}{dr} C_{in}^{Na} \right) \\ &+ \frac{\delta_8}{\sigma_{in}} \left(P e_{ex} \rho_{ex} u_{ex} + \delta_9 \frac{d}{dr} C_{ex}^K + \delta_{10} \frac{d}{dr} C_{ex}^{Na} - \sigma_{ex} \frac{d}{dr} \phi_{ex} \right). \end{aligned} \quad (18)$$

From Eq. 18, because $P e_{in} = O(\epsilon)$ and order of $\delta_8, \delta_9, \delta_{10}$ in Eqs. 16 and 17, we obtain that

$$\frac{d}{dr} \phi_{in} = O(\epsilon). \quad (19)$$

Meanwhile, from Eq. 14b, we can have

$$\frac{d}{dr} O_{in} = O(\epsilon^2), \quad (20)$$

and in Eq. 14e, we know

$$\frac{d}{dr} C_{in}^{Cl} = \frac{d}{dr} (C_{in}^{Na} + C_{in}^K) + o(\epsilon^2). \quad (21)$$

With Eqs. 20 and 21 and A_{in}/V_{in} as constants, we obtain

$$\frac{d}{dr}C_{in}^{Cl} = O(\epsilon^2). \quad (22)$$

Furthermore, using Eq. 14d and boundary conditions for C_{ex}^{Cl} in Eq. 15 yields

$$C_{in}^{Cl} = C_o^{Na} + C_o^K - \frac{1 + |\bar{z}|}{2} \frac{A_{in}}{V_{in}} + O(\epsilon^2). \quad (23)$$

From the experimental setting of lens (41,51,55), we assume that

$$C_o^{Na} + C_o^K - \frac{1 + |\bar{z}|}{2} \frac{A_{in}}{V_{in}} = O(\epsilon). \quad (24)$$

Therefore,

$$C_{in}^{Cl} = O(\epsilon). \quad (25)$$

In all, we claim that

$$\begin{aligned} J_{in}^{Cl} &= Pe_{in}C_{in}^{Cl}u_{in} - D_{in}^{Cl} \left(\frac{d}{dr}C_{in}^{Cl} + z^{Cl}C_{in}^{Cl} \frac{d}{dr}\phi_{in} \right) \\ &= O(\epsilon^2). \end{aligned} \quad (26)$$

By dropping the terms involving these small parameters, the leading order of water circulation system 14a, 14b, 14c, and 14d is as follows:

$$u_{ex}^0 = -\frac{d}{dr}P_{ex}^0 - \delta_1 \frac{d}{dr}\phi_{ex}^0, \quad (27a)$$

$$\frac{d}{dr}O_{in}^0 = 0, \quad (27b)$$

$$O_{in}^0 - O_{ex}^0 = 0, \quad (27c)$$

$$u_{ex}^0 = -u_{in}^0, \quad (27d)$$

where the superscript “0” denotes the leading-order approximation. From Eq. 27, we deduce $O_{ex}^0 = O_{in}^0$ are constants, and the intracellular and extracellular flow are counterflow. The total charge in the leading-order systems is neutral:

$$\sum_i z^i C_{in}^{i,0} + \bar{z} \frac{A_{in}}{V_{in}} = 0, \quad (28a)$$

$$\sum_i z^i C_{ex}^{i,0} = 0. \quad (28b)$$

Combining constant osmotic pressure and charge neutrality yields

$$O_{ex}^0(r) = O_{in}^0(r) = 2(C_{ex}^{Na,0}(1) + C_{ex}^{K,0}(1)), \quad (29a)$$

$$\frac{dC_{in}^{Cl,0}}{dr} = \frac{dC_{ex}^{Cl,0}}{dr} = 0, \quad (29b)$$

which means $C_{in}^{Cl,0}$ and $C_{ex}^{Cl,0}$ are constants and

$$\frac{dC_l^{Na,0}}{dr} = -\frac{dC_l^{K,0}}{dr}, \quad l \in \{in, ex\}. \quad (30)$$

The leading order of potassium and chloride concentrations satisfy

$$\frac{1}{r^2} \frac{d}{dr} (r^2 J_{in}^{K,0}) = 0, \quad (31a)$$

$$\frac{1}{r^2} \frac{d}{dr} (r^2 J_{ex}^{K,0}) = 0, \quad (31b)$$

$$\frac{1}{r^2} \frac{d}{dr} (r^2 J_{ex}^{Cl,0}) = \frac{\mathcal{M}_v^{ex}}{z^{Cl}} (\phi_{in}^0 - \phi_{ex}^0 - E^{Cl,0}), \quad (31c)$$

and

$$\frac{1}{r^2} \frac{d}{dr} (r^2 J_{in}^{Cl,0}) = -\frac{1}{r^2} \frac{d}{dr} (r^2 \delta_8 J_{ex}^{Cl,0}), \quad (31d)$$

where $J_l^{i,0} = Pe_l C_l^{i,0} u_l^0 - D_l^i (d/dr C_l^{i,0} + z^i C_l^{i,0} d/dr \phi_l^0)$ with $i = K, Cl$ and $l = in, ex$, $E^{Cl,0} = \frac{1}{z^{Cl}} \log(C_{ex}^{Cl,0}/C_{in}^{Cl,0})$.

For the electric potential, using the homogeneous Neumann boundary condition at $r = 0$ and Eqs. 29a, 29b, 30, and 14l yields

$$\begin{aligned} \frac{d}{dr}\phi_{in} &= \frac{1}{\sigma_{in}} \left(Pe_{in} \rho_{in} u_{in} + \delta_9 \frac{d}{dr} C_{in}^K + \delta_{10} \frac{d}{dr} C_{in}^{Na} \right) \\ &+ \frac{\delta_8}{\sigma_{in}} \left(Pe_{ex} \rho_{ex} u_{ex} + \delta_9 \frac{d}{dr} C_{ex}^K + \delta_{10} \frac{d}{dr} C_{ex}^{Na} - \sigma_{ex} \frac{d}{dr} \phi_{ex} \right). \end{aligned} \quad (32)$$

At the same time, based on the intracellular equation of potassium (Eq. 14j), the homogeneous Neumann boundary condition at $r = 0$, and Eqs. 29a, 29b, and 30, we have

$$D_{in}^K \frac{d}{dr} C_{in}^K = \left(Pe_{in} C_{in}^K u_{in} - D_{in}^K z^K C_{in}^K \frac{d}{dr} \phi_{in} \right). \quad (33)$$

Substituting Eq. 32 into Eq. 33 yields

$$\begin{aligned} &\left(1 - z^K C_{in}^K \frac{\delta_{10}}{\sigma_{in}} \right) D_{in}^K \frac{dC_{in}^K}{dr} \\ &= \left(\left(1 - z^K D_{in}^K \frac{\rho_{in}}{\sigma_{in}} \right) Pe_{in} u_{in} + z^K D_{in}^K \frac{\delta_8 \sigma_{ex}}{\sigma_{in}} \frac{d\phi_{ex}}{dr} \right) C_{in}^K \\ &\quad + O(\epsilon^2), \end{aligned} \quad (34)$$

where we used the fact that $\rho_{ex} = o(\epsilon^2)$, $\delta_9 = O(\epsilon^2)$, and $dC_l^K/dr = -dC_l^{Na}/dr + O(\epsilon^2)$, $l \in \{in, ex\}$. Because $Pe_{in} = O(\epsilon)$ and $\delta_8 = O(\epsilon)$, in Eq. 34, we claim

$$\frac{dC_{in}^K}{dr} = O(\epsilon). \quad (35)$$

Combining Eqs. 32 and 35 yields the leading-order approximation of intracellular potential

$$\frac{d}{dr}\phi_{in}^0 = \frac{1}{\sigma_{in}^0} Pe_{in}\rho_0 u_{in}^0 - \frac{\delta_8}{\sigma_{in}^0} \sigma_{ex}^0 \frac{d}{dr}\phi_{ex}^0 = O(\epsilon), \quad (36)$$

where $\sigma_{in}^0 = \sum_i D_{in}^i(z^i)^2 C_{in}^{i,0}$, $\sigma_{ex}^0 = \sum_i D_{ex}^i(z^i)^2 C_{ex}^{i,0}$.

Similarly, the leading-order approximation of extracellular potential is

$$\begin{aligned} & -\frac{1}{r^2} \frac{d}{dr} \left(r^2 \left(\delta_{10} \frac{d}{dr} C_{ex}^{Na,0} + \sigma_{ex}^0 \frac{d}{dr} \phi_{ex}^0 \right) \right), \quad (37) \\ & = \mathcal{M}_v^{ex} (2(\phi_{in}^0 - \phi_{ex}^0) - E^{Na,0} - E^{Cl,0}) \end{aligned}$$

where $E^{Na,0} = \frac{1}{z^{Na}} \log(C_{ex}^{Na,0}/C_{in}^{Na,0})$.

To summarize, the leading-order approximation of system 14a, 14b, 14c, 14d, 14e, 14f, 14g, 14h, 14i, 14j, 14k, 14l, and 15 is given by, in domain $\Omega = [0, 1]$,

$$u_{ex}^0 = -\frac{d}{dr} P_{ex}^0 - \delta_1 \frac{d}{dr} \phi_{ex}^0, \quad (38a)$$

$$\frac{d}{dr} O_{in}^0 = 0, \quad (38b)$$

$$O_{in}^0 - O_{ex}^0 = 0, \quad (38c)$$

$$u_{ex}^0 = -u_{in}^0, \quad (38d)$$

$$\sum_i z^i C_{in}^{i,0} + \bar{z} \frac{A_{in}}{V_{in}} = 0, \quad (38e)$$

$$\sum_i z^i C_{ex}^{i,0} = 0 \quad (38f)$$

$$\frac{1}{r^2} \frac{d}{dr} (r^2 J_{in}^{K,0}) = 0, \quad (38g)$$

$$\frac{1}{r^2} \frac{d}{dr} (r^2 J_{ex}^{K,0}) = 0, \quad (38h)$$

$$\frac{1}{r^2} \frac{d}{dr} (r^2 J_{ex}^{Cl,0}) = \frac{\mathcal{M}_v^{ex}}{z^{Cl}} (\phi_{in}^0 - \phi_{ex}^0 - E^{Cl,0}), \quad (38i)$$

$$\frac{1}{r^2} \frac{d}{dr} (r^2 J_{in}^{Cl,0}) = -\frac{1}{r^2} \frac{d}{dr} (r^2 \delta_8 J_{ex}^{Cl,0}), \quad (38j)$$

$$\frac{d}{dr} \phi_{in}^0 = \frac{1}{\sigma_{in}^0} Pe_{in}\rho_0 u_{in}^0 - \frac{\delta_8}{\sigma_{in}^0} \sigma_{ex}^0 \frac{d}{dr} \phi_{ex}^0, \quad (38k)$$

$$\begin{aligned} & -\frac{1}{r^2} \frac{d}{dr} \left(r^2 \left(\delta_{10} \frac{d}{dr} C_{ex}^{Na,0} + \sigma_{ex}^0 \frac{d}{dr} \phi_{ex}^0 \right) \right), \quad (38l) \\ & = \mathcal{M}_v^{ex} (2(\phi_{in}^0 - \phi_{ex}^0) - E^{Na,0} - E^{Cl,0}) \end{aligned}$$

with boundary conditions at $r = 1$

$$\left\{ \begin{aligned} P_{ex}^0 &= 0, C_{ex}^{Cl,0} = C_o^{Na} + C_o^K, C_{ex}^{K,0} = C_o^K, \\ Pe_{in} C_{in}^{K,0} u_{in}^0 - D_{in}^K \left(\frac{d}{dr} C_{in}^{K,0} + z^K C_{in}^{K,0} \frac{d}{dr} \phi_{in}^0 \right) \\ &= \frac{R_s}{z^K} (\phi_{in}^0 - E^{K,0}) - a^K, \\ Pe_{in} \rho_0 u_{in}^0 + \delta_{10} \frac{d}{dr} C_{in}^{Na,0} - \sigma_{in} \frac{d}{dr} \phi_{in}^0 \\ &= \frac{R_s}{z^K} (\phi_{in}^0 - E^{K,0}) + I_p^e, \\ \phi_{ex}^0 &= 0. \end{aligned} \right. \quad (39)$$

In the following, we will further simplify Eqs. 38a, 38b, 38c, 38d, 38e, 38f, 38g, 38h, 38i, 38j, 38k, 38l, and 39 and obtain the relationships between ϕ_{ex}^0 and other leading-order variables by using assumptions concerning the boundary conditions.

Relation between ϕ_{in}^0 and ϕ_{ex}^0

Combining Eqs. 38a, 38d, and 38k and integrating with respect to r yields the relation between ϕ_{in}^0 and ϕ_{ex}^0 as

$$\begin{aligned} \phi_{in}^0(r) &= \left(\frac{Pe_{in}\rho_0\delta_1}{\sigma_{in}^0} - \frac{\delta_8\sigma_{ex}^0}{\sigma_{in}^0} \right) \phi_{ex}^0(r) \\ &+ \frac{Pe_{in}\rho_0}{\sigma_{in}^0} P_{ex}^0(r) + \phi_{in}^0(1), \quad (40) \end{aligned}$$

where we used the boundary conditions $\phi_{ex}^0(1) = P_{ex}^0(1) = 0$.

Relation between P_{ex}^0 and ϕ_{ex}^0

By the homogeneous Neumann boundary condition on $r = 0$ and Eq. 38j, we have

$$J_{in}^{Cl,0} + \delta_8 J_{ex}^{Cl,0} = 0. \quad (41)$$

By Eq. 29b, we can divide Eq. 41 by $C_{ex}^{Cl,0}$ on both sides, and we get

$$\begin{aligned} & \left(Pe_{in} \frac{C_{in}^{Cl,0}}{C_{ex}^{Cl,0}} u_{in}^0 - D_{in}^{Cl} z^{Cl} \frac{C_{in}^{Cl,0}}{C_{ex}^{Cl,0}} \frac{d\phi_{in}^0}{dr} \right) \\ & + \delta_8 \left(Pe_{ex} u_{ex}^0 - D_{ex}^{Cl} z^{Cl} \frac{d\phi_{ex}^0}{dr} \right) = 0 \quad (42) \end{aligned}$$

Based on the charge neutrality Eq. 28, constant osmotic pressure Eq. 29a, and parameters in Appendix B in the Supporting Materials and Methods, we define

$$\delta_{11} = \frac{C_{in}^{Cl,0}}{C_{ex}^{Cl,0}} = \frac{C_o^{Na} + C_o^K - \frac{1+|\bar{z}|}{2} \frac{A_{in}}{V_{in}}}{C_o^{Cl,0}} = O(\epsilon). \quad (43)$$

Then, combining Eq. 36 and $Pe_{in} = O(\epsilon)$, Eq. 42 yields the following equation by omitting the higher-order terms:

$$Pe_{ex} u_{ex}^0 - D_{ex}^{Cl} z^{Cl} \frac{d\phi_{ex}^0}{dr} = 0. \quad (44)$$

Finally, by using the boundary condition, we have the relation between extracellular pressure and electric potential as

$$P_{ex}^0 = \frac{D_{ex}^{Cl} - Pe_{ex}\delta_1}{Pe_{ex}}\phi_{ex}^0. \quad (45)$$

Expression of E^{Na}

Based on potassium equation and relation in Eqs. 40 and 45, we have the expression for C_{in}^K and C_{ex}^K as

$$C_{ex}^{K,0} = C_0^{K,0} \exp\left(-\left(1 + \frac{D_{ex}^{Cl}}{D_{ex}^K}\right)\phi_{ex}^0\right), \quad (46a)$$

$$C_{in}^{K,0} = C_{in}^{K,0}(1) \exp\left(\left(\frac{Pe_{in}D_{ex}^{Cl}}{Pe_{ex}D_{in}^K} - \frac{Pe_{in}D_{ex}^{Cl}\rho_0}{Pe_{ex}\sigma_{in}^0}\right)\phi_{ex}^0\right) \exp\left(\left(\frac{\delta_9\sigma_{ex}^0}{\sigma_{in}^0}\right)\phi_{ex}^0\right), \quad (46b)$$

where

$$C_{in}^{K,0}(1) = C_o^{K,0} \exp\left(\frac{a^K}{R_s} - \phi_{in}(1)\right). \quad (47)$$

Based on Eq. 28, we can get

$$E^{Na,0} = \frac{1}{z^{Na}} \log\left(\frac{C_{ex}^{Na,0}}{C_{in}^{Na,0}}\right) = \frac{1}{z^{Na}} \log\left(\frac{C_{ex}^{Cl,0} - C_{ex}^{K,0}}{C_{in}^{Cl,0} + \left|\bar{z}\right| \frac{A_{in}}{V_{in}} - C_{in}^{K,0}}\right). \quad (48)$$

Extracellular electric potential system

By Eqs. 40 and 45, we have ϕ_{in} as

$$\phi_{in}^0(r) = \left(\frac{D_{ex}^{Cl}Pe_{in}\rho_0}{\sigma_{in}^0Pe_{ex}} - \frac{\delta_9\sigma_{ex}^0}{\sigma_{in}^0}\right)\phi_{ex}^0(r) + \phi_{in}^0(1). \quad (49)$$

The value $\phi_{in}^0(1)$ is determined by the boundary condition of ϕ_{in}^0 in Eq. 39, where

$$-\mathcal{M}_v^{in} \int_0^1 (2(\phi_{in}^0 - \phi_{ex}^0) - E^{Na,0} - E^{Cl,0})s^2 ds = a^{Na}, \quad (50)$$

where we use

$$a^{Na} = -a^K + I_p^\phi, \quad \frac{R_s}{z^K}(\phi_{in} - E^K) = -a^K.$$

To summarize, we obtained the simplified model of system 38a, 38b, 38c, 38d, 38e, 38f, 38g, 38h, 38i, 38j, 38k, 38l, and 39 as follows:

$$-\frac{1}{r^2} \frac{d}{dr} \left(r^2 \left(\delta_{10} \frac{d}{dr} C_{ex}^{Na,0} + \sigma_{ex}^0 \frac{d}{dr} \phi_{ex}^0 \right) \right), \quad (51a)$$

$$= \mathcal{M}_v^{ex} (2(\phi_{in}^0 - \phi_{ex}^0) - E^{Na,0} - E^{Cl,0})$$

$$\phi_{in}^0(r) = \left(\frac{D_{ex}^{Cl}Pe_{in}\rho_0}{\sigma_{in}^0Pe_{ex}} - \frac{\delta_9\sigma_{ex}^0}{\sigma_{in}^0} \right) \phi_{ex}^0(r) + \phi_{in}^0(1), \quad (51b)$$

$$-\mathcal{M}_v^{in} \int_0^1 (2(\phi_{in}^0 - \phi_{ex}^0) - E^{Na,0} - E^{Cl,0})s^2 ds, \quad (51c)$$

$$= a^{Na}$$

$$u_{ex}^0 = -\frac{d}{dr} P_{ex}^0 - \delta_1 \frac{d}{dr} \phi_{ex}^0, \quad (51d)$$

$$u_{in}^0 = -u_{ex}^0, \quad (51e)$$

$$C_{ex}^{K,0} = C_0^{K,0} \exp\left(-\left(1 + \frac{D_{ex}^{Cl}}{D_{ex}^K}\right)\phi_{ex}^0\right), \quad (51f)$$

$$C_{in}^{K,0} = C_{in}^{K,0}(1) \exp\left(\left(\frac{Pe_{in}D_{ex}^{Cl}}{Pe_{ex}D_{in}^K} - \frac{Pe_{in}D_{ex}^{Cl}\rho_0}{Pe_{ex}\sigma_{in}^0}\right)\phi_{ex}^0\right) \exp\left(\left(\frac{\delta_9\sigma_{ex}^0}{\sigma_{in}^0}\right)\phi_{ex}^0\right), \quad (51g)$$

$$C_{ex}^{Na,0} = C_{ex}^{Cl,0} - C_{ex}^{K,0}, \quad (51h)$$

$$C_{in}^{Na,0} = C_{in}^{Cl,0} + \frac{A_{in}}{V_{in}} - C_{in}^{K,0}, \quad (51i)$$

$$C_{in}^{Cl,0} = C_o^{Na,0} + C_o^{K,0} - \frac{1 + |\bar{z}|}{2} \frac{A_{in}}{V_{in}}, \quad (51j)$$

$$C_{ex}^{Cl,0} = C_o^{Na,0} + C_o^{K,0}, \quad (51k)$$

$$P_{ex}^0 = \frac{D_{ex}^{Cl} - Pe_{ex}\delta_1}{Pe_{ex}}\phi_{ex}^0, \quad (51l)$$

with boundary conditions

$$\begin{cases} \frac{d\phi_{ex}^0}{dr} = 0, & \text{at } r = 0, \\ \phi_{ex}^0 = 0, & \text{at } r = 1. \end{cases} \quad (52)$$

Under the same assumptions in (51)—for example, uniform diffusion constants for all ions and constant Nernst potential—our simplified model system 51 recovers the model proposed by Mathias. The main contribution here is that we remove the assumptions that Nernst potentials and effective conductance should be constants. By using the relationships between ion concentrations and external potential, we obtain the space-dependent

Nernst potential, which yields a much better approximation to the full model (see Fig. 4).

RESULTS AND DISCUSSION

In this section, we present numerical simulations using both the full and simplified models. The finite volume method (70) is used to preserve mass conservation of ions. The convex iteration (72) is employed to solve the nonlinear coupled system. The numerical algorithm is implemented in MATLAB (The MathWorks, Natick, MA).

Model calibration: Membrane conductance effects intracellular hydrostatic pressure

In this section, we first calibrate the full model by comparison with the experimental data to study the effect of connexin on intracellular hydrostatic pressure.

Intracellular hydrostatic pressure is an important physiological quantity (63). In some studies (28,47), the authors showed that the connexin (gap-junction; see Fig. 1, D and E) conductance plays an important role in the microcirculation of lens. It is said that if the intracellular conductance κ_{in}/μ_{in} in lenses is approximately doubled, the hydrostatic pressure gradient in the lenses should become approximately half of the original one. In this section, we calibrate our model. We choose a value of the intracellular conductance (κ_{in}/μ_{in}) that correctly calculates the experimental results in (28,47).

In Fig. 3 A, the value $\kappa_{in}^w = 4.6830 \times 10^{-20}/m^2$ (black line) yields a good approximation to experimental data (blue markers). When the conductivity of the connexins is doubled so that parameter value κ_{in} is $2\kappa_{in}^w$ (in the lens of mice Cx46 knock-in [KI] lens) as in the experiments (28,47), which doubled the conductivity of the connexins by using Cx46 KI mice lens, our model (black dot) can also match the experimental data (red markers): the intracellular hydrostatic pressure drops to half. This result shows that our full model can correctly predict the effect of permeability of membrane on hydrostatic pressure.

Interestingly, Fig. 3, B–D show that other intracellular quantities and extracellular ones (Supporting Materials and Methods) are insensitive to increases in the permeability by a factor of 20, even to $20\kappa_{in}^w$. The reason for this can be explained by using our simplified system 51. If the variation of intracellular conductance still keeps the δ_2 to be a small quantity in the dimensionless system 14, our simplified model will be still valid. In the simplified model, all the quantities except intracellular hydrostatic pressure are related to the extracellular electric potential. However, the extracellular electric potential will not be affected by the change of the intracellular conductance because Eq. 51a does not involve intracellular conductance.

Full model versus simplified model

In this section, we compare the full model 14a, 14b, 14c, 14d, 14e, 14f, 14g, 14h, 14i, 14j, 14k, 14l, and 15 with the

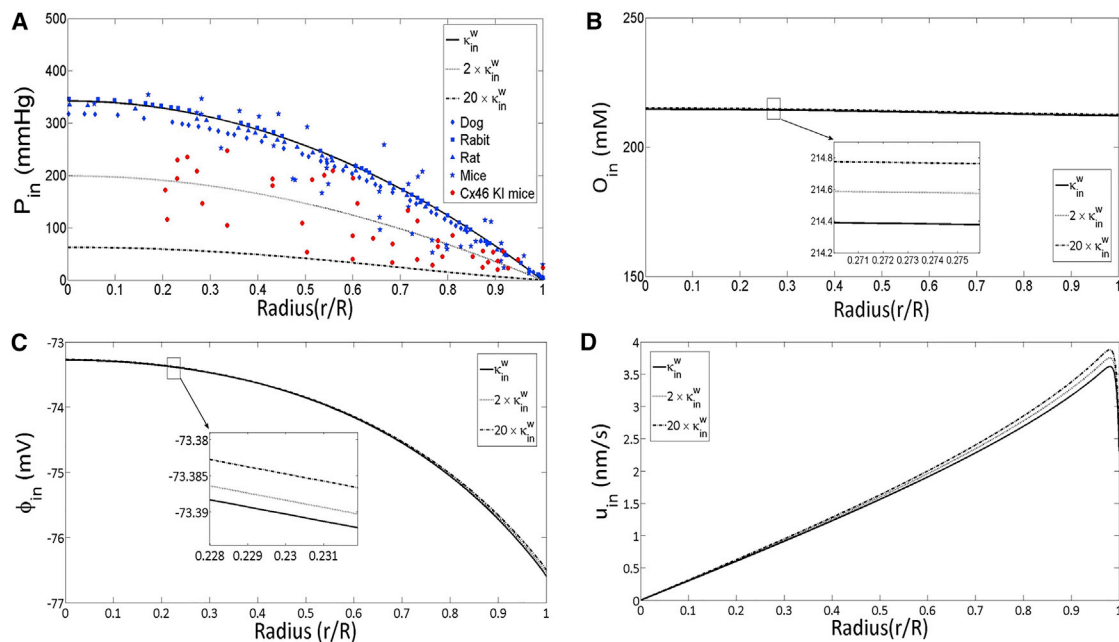


FIGURE 3 Comparison between different κ_{in} . (A) Comparison between simulation results and experimental results. The experimental data of dog, rabbit, and rat come from (47). Mice and Cx46 KI mice come from (28). According to (28), the Cx46 KI mice lens has twice the number density of lens gap-junction channels compared to mice. The parameter $\kappa_{in}^w = 4.6830 \times 10^{-20}/m^2$, and radius is written in dimensionless units for different species. (B) Space distribution of intracellular osmotic pressure (O_{in}). (C) Space distribution of intracellular electric potential (ϕ_{in}). (D) Space distribution of intracellular water velocity (u_{in}). To see this figure in color, go online.

simplified model 51 and Mathias model in (51). The numerical results of full model (*black lines*) in Fig. 4, A–C suggest that the variations in intracellular electric potential, extracellular conductance, and Nernst potential of Cl^- are rather small. The assumption of constant values for those variables (potential, extracellular conductance, and Nernst, i.e., chemical potential of Cl^-) in the Mathias model (shown as *red dash-dot lines*) is reason-

able. However, the Nernst potentials of sodium and potassium (Fig. 4, D and E) have large variations because of the effect of sodium-potassium pump. Our simplified model (*blue dash lines*) describes these variations with small errors. The comparisons for extracellular pressure, velocity, and potential (Fig. 4, F–H) confirm that our simplified model yields good approximations to the full model.

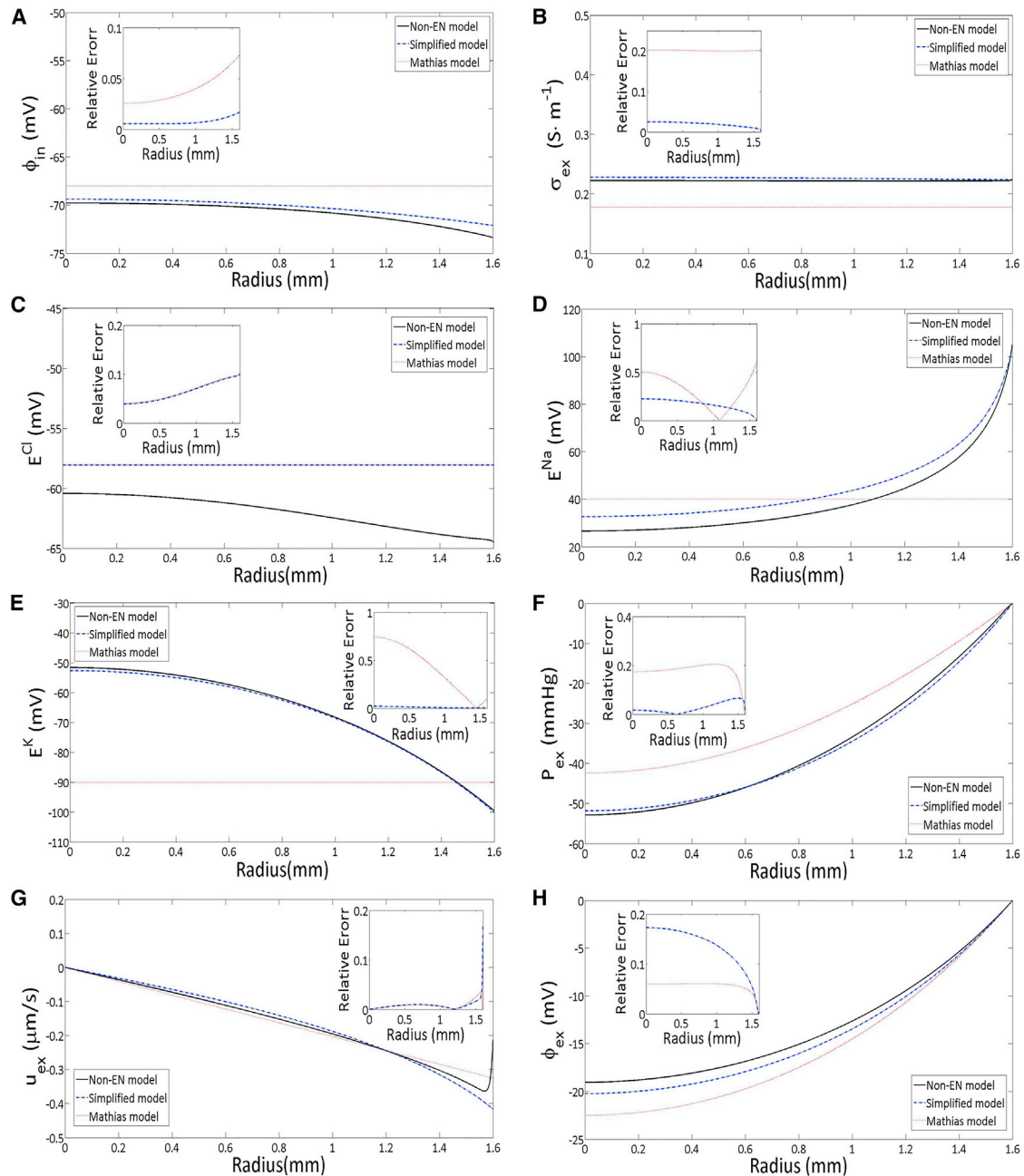


FIGURE 4 Comparison of electroneutral and simplified and the Mathias model in (51). (A) Space distribution of intracellular electric potential (ϕ_{in}). (B) Space distribution of extracellular conductance (σ_{ex}). (C) Space distribution of chloride nernst potential (E^{Cl}). (D) Space distribution of sodium nernst potential (E^{Na}). (E) Space distribution of potassium nernst potential (E^K). (F) Space distribution of extracellular pressure (P_{ex}). (G) Space distribution of extracellular velocity (u_{ex}). (H) Space distribution of extracellular electric potential (ϕ_{ex}). To see this figure in color, go online.

CONCLUSIONS

In this work, we propose a bidomain model to study the microcirculation of lens. We include a capacitor in the representation of the membrane, and so our model is consistent with classical electrodynamics. Consistency produces a linear correction term in the classical charge neutrality equation. This full model is calibrated by comparison with the experiment studying effect of connexin on hydrostatic pressure. By changing only the intracellular membrane conductance (strength of connection), our model could match the two experimental results with different connexins very well. Our model is capable of making predictions about the circulation of the lens. Furthermore, the numerical simulations show that the velocity, potential, and osmotic pressure in the intra- and extracellular spaces are not sensitive to increasing intracellular membrane conductance.

Based on the asymptotic analysis, we proposed a simplified model that allows us to obtain a deep understanding of the physical process without making unrealistic assumptions. Our results showed that the simplified model is a good approximation of the full model in which Nernst potentials and conductivity vary significantly inside the lens.

Our model allows calculation of variables that determine the role and life of the lens as an organ. Particularly important are the factors that determine the transparency of the lens because that is the main function of the organ. The dependence of the size of the extracellular space, and thus the pressure in extracellular and intracellular spaces and the difference between those two, is likely to be an important determinant of transparency. One imagines that swelling of the extracellular space will scatter light, particularly because the swelling is likely to be irregular (in a way our model does not yet capture). Changes in the osmolarity (i.e., activity of water estimated by the total concentration of solutes) are likely to be important as well.

This hydrodynamic bidomain model can point the way to dealing with other cells, tissues, and organs in which current flow, water flow, and cell-volume changes are important. These include the kidney, the central nervous system (where the narrow extracellular space poses many of the biological problems facing the lens), the t-tubular system of skeletal and much cardiac muscle, and so on. We show that a mathematically well-defined model can deal with the reality of biological structure and its complex distribution of channels, etc.

Conservation laws applied to simplified structures are enough to provide quite useful results because they were in three-dimensional electrical problems of cells of various geometries (16) and syncytia (3,23). The exact results are analyzed with perturbation methods, described in general in (73), and these methods allow dramatic simplifications without introducing large or even significant errors. It is as if evolution chose systems in which parameters and structures allow simple results and in which parameters can control biological function robustly.

Of course, we only point the way. Additional compartments and additional structural complexity will surely be needed to deal with the workings of evolution. But these can be handled in a mathematically defined way, yielding approximate results with clear physical and biological interpretation. By combining the multidomain model and membrane potential dependent conductances, one can model depolarization induced by extra potassium in the lens (53,55) and the cortical spreading depression problem (71,74,75). The ultimate goals will be 1) to provide as much precision in the mathematics and physics as we can, starting from first principles (62), and 2) to provide a general basis for treatments of convection in other tissues that involve microcirculation. Computational models of these are not in hand and may be hard to construct because so little is known of those systems compared to the lens. With what we have learned here, we hope a general mathematical approach and model of the type we present here may be constructed and prove helpful in other systems with narrow extracellular spaces that are likely to need microcirculation to augment diffusion, such as cardiac and skeletal muscle, kidney, liver, epithelia, and the extracellular space of the brain.

SUPPORTING MATERIAL

Supporting Materials and Methods, one figure, and two tables are available at [http://www.biophysj.org/biophysj/supplemental/S0006-3495\(19\)30134-1](http://www.biophysj.org/biophysj/supplemental/S0006-3495(19)30134-1).

AUTHOR CONTRIBUTIONS

Y.Z., S.X., and H.H. did the model derivations and carried out the numerical simulations. R.S.E. and H.H. designed the study, coordinated the study, and commented on the manuscript. All authors gave final approval for publication.

ACKNOWLEDGMENTS

This research is supported in part by the Fields Institute for Research in Mathematical Science (S.X., R.S.E., and H.H.) and the Natural Sciences and Engineering Research Council of Canada (H.H.). R.S.E. is grateful for the support of the Fields Institute in the form of a Fields Research Fellowship.

REFERENCES

1. Eisenberg, R. S., and J. L. Rae. 1976. Current-voltage relationships in the crystalline lens. *J. Physiol.* 262:285–300.
2. Eisenberg, R. 2018. Electrical structure of biological cells and tissues: impedance spectroscopy, stereology, and singular perturbation theory. *In Impedance Spectroscopy: Theory, Experiment, and Applications*, Third Edition. E. Barsoukov and J. Ross Macdonald, eds. Wiley-Interscience, pp. 472–478.
3. Eisenberg, B. R. 1979. Skeletal muscle fibers: stereology applied to anisotropic and periodic structures. *In Stereological Methods: Practical Methods for Biological Morphometry* E. R. Weibel, ed. Academic Press, pp. 274–284.

4. Barsoukov, E., and J. R. Macdonald. 2018. Impedance Spectroscopy: Theory, Experiment, and Applications, Third Edition. John Wiley & Sons, Hoboken, NJ.
5. Eisenberg, R. S. 1980. Structural complexity, circuit models, and ion accumulation. *Fed. Proc.* 39:1540–1543.
6. Eisenberg, R. S. 1983. Impedance measurement of the electrical structure of skeletal muscle. *Handbook of Physiology*. American Physiological Society, pp. 301–323.
7. Eisenberg, R. S., and R. T. Mathias. 1980. Structural analysis of electrical properties of cells and tissues. *Crit. Rev. Bioeng.* 4:203–232.
8. Eisenberg, R. S., R. T. Mathias, and J. S. Rae. 1977. Measurement, modeling, and analysis of the linear electrical properties of cells. *Ann. N. Y. Acad. Sci.* 303:342–354.
9. Eisenberg, R. S. 1984. Membranes and channels physiology and molecular biology. In *Membranes, Channels, and Noise*. R. S. Eisenberg, M. Frank, and C. F. Stevens, eds. Plenum Press, pp. 235–283.
10. Mathias, R. T. 1984. Analysis of membrane properties using extrinsic noise. In *Membranes, Channels, and Noise*. R. S. Eisenberg, M. Frank, and C. F. Stevens, eds. Plenum Press, pp. 49–116.
11. Ebihara, L., and R. T. Mathias. 1985. Linear impedance studies of voltage-dependent conductances in tissue cultured chick heart cells. *Biophys. J.* 48:449–460.
12. Levis, R. A., R. T. Mathias, and R. S. Eisenberg. 1983. Electrical properties of sheep Purkinje strands. Electrical and chemical potentials in the clefts. *Biophys. J.* 44:225–248.
13. Mathias, R. T., L. Ebihara, ..., E. A. Johnson. 1981. Linear electrical properties of passive and active currents in spherical heart cell clusters. *Biophys. J.* 36:221–242.
14. Milton, R. L., R. T. Mathias, and R. S. Eisenberg. 1985. Electrical properties of the myotendon region of frog twitch muscle fibers measured in the frequency domain. *Biophys. J.* 48:253–267.
15. Valdiosera, R., C. Clausen, and R. S. Eisenberg. 1974. Measurement of the impedance of frog skeletal muscle fibers. *Biophys. J.* 14:295–315.
16. Barcion, V., J. Cole, and R. S. Eisenberg. 1971. A singular perturbation analysis of induced electric fields in nerve cells. *SIAM J. Appl. Math.* 21:339–354.
17. Eisenberg, R. S., V. Barcion, and R. T. Mathias. 1979. Electrical properties of spherical syncytia. *Biophys. J.* 25:151–180.
18. Mathias, R. T., J. L. Rae, and R. S. Eisenberg. 1979. Electrical properties of structural components of the crystalline lens. *Biophys. J.* 25:181–201.
19. Mathias, R. T., J. L. Rae, and R. S. Eisenberg. 1981. The lens as a nonuniform spherical syncytium. *Biophys. J.* 34:61–83.
20. Rae, J. L., R. T. Mathias, and R. S. Eisenberg. 1982. Physiological role of the membranes and extracellular space with the ocular lens. *Exp. Eye Res.* 35:471–489.
21. Mathias, R. T., R. S. Eisenberg, and R. Valdiosera. 1977. Electrical properties of frog skeletal muscle fibers interpreted with a mesh model of the tubular system. *Biophys. J.* 17:57–93.
22. Valdiosera, R., C. Clausen, and R. S. Eisenberg. 1974. Impedance of frog skeletal muscle fibers in various solutions. *J. Gen. Physiol.* 63:460–491.
23. Rae, J. L., R. D. Thomson, and R. S. Eisenberg. 1982. The effect of 2-4 dinitrophenol on cell to cell communication in the frog lens. *Exp. Eye Res.* 35:597–609.
24. Baldo, G. J., X. Gong, ..., R. T. Mathias. 2001. Gap junctional coupling in lenses from alpha(8) connexin knockout mice. *J. Gen. Physiol.* 118:447–456.
25. Donaldson, P. J., L. S. Musil, and R. T. Mathias. 2010. Point: a critical appraisal of the lens circulation model—an experimental paradigm for understanding the maintenance of lens transparency? *Invest. Ophthalmol. Vis. Sci.* 51:2303–2306.
26. Donaldson, P., J. Kistler, and R. T. Mathias. 2001. Molecular solutions to mammalian lens transparency. *News Physiol. Sci.* 16:118–123.
27. Gao, J., X. Sun, ..., R. T. Mathias. 2004. Connections between connexins, calcium, and cataracts in the lens. *J. Gen. Physiol.* 124:289–300.
28. Gao, J., X. Sun, ..., R. T. Mathias. 2011. Lens intracellular hydrostatic pressure is generated by the circulation of sodium and modulated by gap junction coupling. *J. Gen. Physiol.* 137:507–520.
29. Gao, J., X. Sun, ..., R. T. Mathias. 2000. Isoform-specific function and distribution of Na/K pumps in the frog lens epithelium. *J. Membr. Biol.* 178:89–101.
30. Mathias, R. T., J. Kistler, and P. Donaldson. 2007. The lens circulation. *J. Membr. Biol.* 216:1–16.
31. Mathias, R. T., and J. L. Rae. 1985. Transport properties of the lens. *Am. J. Physiol.* 249:C181–C190.
32. Mathias, R. T., and J. L. Rae. 2004. The lens: local transport and global transparency. *Exp. Eye Res.* 78:689–698.
33. Mathias, R. T., J. L. Rae, and G. J. Baldo. 1997. Physiological properties of the normal lens. *Physiol. Rev.* 77:21–50.
34. Mathias, R. T., G. Riquelme, and J. L. Rae. 1991. Cell to cell communication and pH in the frog lens. *J. Gen. Physiol.* 98:1085–1103.
35. Mathias, R. T., and H. Wang. 2005. Local osmosis and isotonic transport. *J. Membr. Biol.* 208:39–53.
36. Mathias, R. T., T. W. White, and X. Gong. 2010. Lens gap junctions in growth, differentiation, and homeostasis. *Physiol. Rev.* 90:179–206.
37. McNulty, R., H. Wang, ..., S. Bassnett. 2004. Regulation of tissue oxygen levels in the mammalian lens. *J. Physiol.* 559:883–898.
38. Rae, J. L., C. Bartling, ..., R. T. Mathias. 1996. Dye transfer between cells of the lens. *J. Membr. Biol.* 150:89–103.
39. Varadaraj, K., S. Kumari, ..., R. T. Mathias. 2005. Regulation of aquaporin water permeability in the lens. *Invest. Ophthalmol. Vis. Sci.* 46:1393–1402.
40. Varadaraj, K., C. Kushmerick, ..., R. T. Mathias. 1999. The role of MIP in lens fiber cell membrane transport. *J. Membr. Biol.* 170:191–203.
41. Vaghefi, E., D. T. Malcolm, ..., P. J. Donaldson. 2012. Development of a 3D finite element model of lens microcirculation. *Biomed. Eng. Online.* 11:69.
42. Vaghefi, E., B. P. Pontre, ..., P. J. Donaldson. 2011. Visualizing ocular lens fluid dynamics using MRI: manipulation of steady state water content and water fluxes. *Am. J. Physiol. Regul. Integr. Comp. Physiol.* 301:R335–R342.
43. Vaghefi, E., N. Liu, and P. J. Donaldson. 2013. A computer model of lens structure and function predicts experimental changes to steady state properties and circulating currents. *Biomed. Eng. Online.* 12:85.
44. Wu, H. T., P. J. Donaldson, and E. Vaghefi. 2016. Review of the experimental background and implementation of computational models of the ocular lens microcirculation. *IEEE Rev. Biomed. Eng.* 9:163–176.
45. Donaldson, P. J. 2012. Fluid in equals fluid out—evidence for circulating fluid fluxes in the lens. *Invest. Ophthalmol. Vis. Sci.* 53:7727.
46. Donaldson, P. J., A. C. Grey, ..., E. Vaghefi. 2017. The physiological optics of the lens. *Prog. Retin. Eye Res.* 56:e1–e24.
47. Gao, J., X. Sun, ..., R. T. Mathias. 2013. The effect of size and species on lens intracellular hydrostatic pressure. *Invest. Ophthalmol. Vis. Sci.* 54:183–192.
48. Schey, K. L., R. S. Petrova, ..., P. J. Donaldson. 2017. The role of aquaporins in ocular lens homeostasis. *Int. J. Mol. Sci.* 18:E2693.
49. Vaghefi, E., A. Kim, and P. J. Donaldson. 2015. Active maintenance of the gradient of refractive index is required to sustain the optical properties of the lens. *Invest. Ophthalmol. Vis. Sci.* 56:7195–7208.
50. Mathias, R. T. 1985. Epithelial water transport in a balanced gradient system. *Biophys. J.* 47:823–836.
51. Mathias, R. T. 1985. Steady-state voltages, ion fluxes, and volume regulation in syncytial tissues. *Biophys. J.* 48:435–448.
52. Baldo, G. J., and R. T. Mathias. 1992. Spatial variations in membrane properties in the intact rat lens. *Biophys. J.* 63:518–529.

53. Delamere, N. A., and G. Duncan. 1977. A comparison of ion concentrations, potentials and conductances of amphibian, bovine and cephalopod lenses. *J. Physiol.* 272:167–186.
54. Mathias, R. T., and J. L. Rae. 1985. Steady state voltages in the frog lens. *Curr. Eye Res.* 4:421–430.
55. Malcolm, D. T. K. 2006. A computational model of the ocular lens. PhD thesis (ResearchSpace@ Auckland).
56. Currie, I. G., and I. Currie. 2002. *Fundamental Mechanics of Fluids, Third Edition.* CRC Press, New York.
57. Ferziger, J. H., and M. Peric. 2012. *Computational Methods for Fluid Dynamics.* Springer Science & Business Media, Berlin, Germany.
58. Duncan, G., K. R. Hightower, ..., G. Maraini. 1989. Human lens membrane cation permeability increases with age. *Invest. Ophthalmol. Vis. Sci.* 30:1855–1859.
59. DeRosa, A. M., F. J. Martinez-Wittinghan, ..., T. W. White. 2005. Intercellular communication in lens development and disease. In *Gap Junctions in Development and Disease.* E. Winterhager, ed. Springer, pp. 173–195.
60. Shiels, A., D. Mackay, ..., S. Bhattacharya. 1998. A missense mutation in the human connexin50 gene (GJA8) underlies autosomal dominant “zonular pulverulent” cataract, on chromosome 1q. *Am. J. Hum. Genet.* 62:526–532.
61. Mackay, D., A. Ionides, ..., S. Bhattacharya. 1999. Connexin46 mutations in autosomal dominant congenital cataract. *Am. J. Hum. Genet.* 64:1357–1364.
62. Xu, S., B. Eisenberg, ..., H. Huang. 2018. Osmosis through a semi-permeable membrane: a consistent approach to interactions. *arXiv*, arXiv:1806.00646 <https://arxiv.org/abs/1806.00646>.
63. Gao, J., X. Sun, ..., R. T. Mathias. 2015. Feedback regulation of intracellular hydrostatic pressure in surface cells of the lens. *Biophys. J.* 109:1830–1839.
64. Levine, O. R., R. B. Mellins, ..., A. P. Fishman. 1967. The application of Starling’s law of capillary exchange to the lungs. *J. Clin. Invest.* 46:934–944.
65. Eisenberg, B. 2012. Life’s solutions are complex fluids. A mathematical challenge. *arXiv*, arXiv:1207.4737 <https://arxiv.org/abs/1207.4737>.
66. Eisenberg, B. 2013. Interacting ions in biophysics: real is not ideal. *Biophys. J.* 104:1849–1866.
67. Wan, L., S. Xu, ..., P. Sheng. 2014. Self-consistent approach to global charge neutrality in electrokinetics: a surface potential trap model. *Phys. Rev. X.* 4:011042.
68. Mobley, B. A., J. Leung, and R. S. Eisenberg. 1974. Longitudinal impedance of skinned frog muscle fibers. *J. Gen. Physiol.* 63:625–637.
69. Mobley, B. A., J. Leung, and R. S. Eisenberg. 1975. Longitudinal impedance of single frog muscle fibers. *J. Gen. Physiol.* 65:97–113.
70. Song, Z., X. Cao, and H. Huang. 2018. Electroneutral models for dynamic Poisson-Nernst-Planck systems. *Phys. Rev. E.* 97:012411.
71. Mori, Y. 2015. A multidomain model for ionic electrodiffusion and osmosis with an application to cortical spreading depression. *Physica D.* 308:94–108.
72. Lee, C.-C., H. Lee, ..., C. Liu. 2010. New Poisson–Boltzmann type equations: one-dimensional solutions. *Nonlinearity.* 24:431–458.
73. Peskoff, A., and R. S. Eisenberg. 1973. Interpretation of some micro-electrode measurements of electrical properties of cells. *Annu. Rev. Biophys. Bioeng.* 2:65–79.
74. Chang, J. C., K. C. Brennan, ..., J. J. Wylie. 2013. A mathematical model of the metabolic and perfusion effects on cortical spreading depression. *PLoS One.* 8:e70469.
75. Yao, W., H. Huang, and R. M. Miura. 2011. A continuum neuronal model for the instigation and propagation of cortical spreading depression. *Bull. Math. Biol.* 73:2773–2790.

Biophysical Journal, Volume 116

Supplemental Information

A Bidomain Model for Lens Microcirculation

Yi Zhu, Shixin Xu, Robert S. Eisenberg, and Huaxiong Huang

Supplementary Information to the paper "A Bidomain Model for Lens Microcirculation"

Y. Zhu, S. Xu, R. S. Eisenberg, H. Huang

Appendix A. Model Parameters

Parameters	Mathias [1]	Malcolm [2]	Parameters	Mathias [1]	Malcolm [2]
R	$1.6 \times 10^{-3} \text{ m}$	$1.6 \times 10^{-3} \text{ m}$	L_m	$3.75 \times 10^{-13} \text{ m}/(\text{Pa} \cdot \text{s})$	$1.34 \times 10^{-13} \text{ m}/(\text{Pa} \cdot \text{s})$
A_{in}/V_{in}	78 mM	78 mM	L_s	$3.75 \times 10^{-13} \text{ m}/(\text{Pa} \cdot \text{s})$	$8.89 \times 10^{-13} \text{ m}/(\text{Pa} \cdot \text{s})$
C_o^{Na}	107 mM	107 mM	\mathcal{M}_{in}	0.988	0.99
C_o^K	3 mM	3 mM	\mathcal{M}_{ex}	0.012	0.01
C_m	-	$1 \times 10^{-2} \text{ F}/\text{m}^2$	\mathcal{M}_v	$6 \times 10^5/\text{m}$	$5 \times 10^5/\text{m}$
D_{ex}^{Na}	-	$1.39 \times 10^{-9} \text{ m}^2/\text{s}$	T	-	310 K
D_{ex}^K	-	$2.04 \times 10^{-9} \text{ m}^2/\text{s}$	k_e	$1.72 \times 10^{-8} \text{ m}^2/(\text{V} \cdot \text{s})$	$1.45 \times 10^{-8} \text{ m}^2/(\text{V} \cdot \text{s})$
D_{ex}^{Cl}	-	$2.12 \times 10^{-9} \text{ m}^2/\text{s}$	k_B	$1.38 \times 10^{-23} \text{ J}/\text{K}$	$1.38 \times 10^{-23} \text{ J}/\text{K}$
D_{in}^{Na}	-	$1.39 \times 10^{-11} \text{ m}^2/\text{s}$	K_{K1}	-	1.6154 mM
D_{in}^K	-	$2.04 \times 10^{-11} \text{ m}^2/\text{s}$	K_{K2}	-	0.1657 mM
D_{in}^{Cl}	-	$2.12 \times 10^{-11} \text{ m}^2/\text{s}$	$K_{Na1,Na2}$	-	2.3393 mM
e	$1.6 \times 10^{-19} \text{ A} \cdot \text{s}$	$1.6 \times 10^{-19} \text{ A} \cdot \text{s}$	η	0.988	0.99
g^{Na}	$2.2 \times 10^{-3} \text{ S}/\text{m}^2$	$2.2 \times 10^{-3} \text{ S}/\text{m}^2$	κ_{ex}	$1.141 \times 10^{-16} \text{ m}^2$	$1.33 \times 10^{-16} \text{ m}^2$
g^{Cl}	$2.2 \times 10^{-3} \text{ S}/\text{m}^2$	$2.2 \times 10^{-3} \text{ S}/\text{m}^2$	κ_{in}	-	$9.366 \times 10^{-19} \text{ m}^2$
G^K	$2.1 \text{ S}/\text{m}^2$	$2.1 \text{ S}/\text{m}^2$	$\gamma_{m,s}$	1	1
I_p	$2.3 \times 10^{-2} \text{ A}/\text{m}^2$	-	τ_c	0.16	0.16
I_{max1}	-	$0.478 \text{ A}/\text{m}^2$	μ	$7 \times 10^{-4} \text{ Pa} \cdot \text{s}$	$7 \times 10^{-4} \text{ Pa} \cdot \text{s}$
I_{max2}	-	$0.065 \text{ A}/\text{m}^2$	\bar{z}	-1.5	-1.5

Appendix B. Dimensionless Parameters and Scales

The following dimensionless parameters' value and scales calculation based on values in [2]

Scales/Parameters	Value	Parameters	Value
a^{Na*}	$6.9 \times 10^{-2} A/m^2$	δ_0	$\frac{1}{99}$
C^*	110 mM	δ_1	1.2031×10^{-1}
O^*	220 mM	δ_2	6.861×10^{-3}
P^*	16.937 KPa	δ_3	2.9894×10^{-2}
u_{in}^*	3.2506 nm/s	δ_4	3.5323×10^{-5}
u_{ex}^*	3.2181 $\mu m/s$	δ_5	4.3022×10^{-3}
ϕ^*	26.7 mV	δ_6	1.2745×10^{-5}
D_{ex}^*	$3.392 \times 10^{10} m^2/s$	δ_7	1.2617×10^{-3}
D_{in}^*	$2.12 \times 10^{-11} m^2/s$	δ_8	1.6162×10^{-1}
Pe_{ex}	1.5180	δ_9	$\frac{125}{110}$
Pe_{in}	2.4533×10^{-1}	δ_{10}	3.443×10^{-1}
$\tilde{D}_{in,ex}^{Na}$	0.6557	δ_{11}	3.77×10^{-2}
$\tilde{D}_{in,ex}^K$	0.9623	ρ_0	$\frac{117}{110}$
$\tilde{D}_{in,ex}^{cl}$	1	$\tilde{\mathcal{M}}_v^{in}$	3.3859×10^{-1}
R_s	4.00×10^{-1}	$\tilde{\mathcal{M}}_v^{ex}$	2.095

Appendix C. Non-dimensionalization

In this section, we derive the dimensionless model based on the lens, which has been widely studied. The major ions we considering here are sodium (Na^+), potassium (K^+) and chloride (Cl^-) and the sodium-potassium pump which distributed on the surface of the lens. Although we restrict ourselves in this particular problem, the following procedure can be applied in a wide range of practical problems in biological syncytia.

Appendix C.1. Water circulation

In the following, we assume the typical length of lens is R . The fluid system is driven by the osmotic gradient, which is generated by the sodium-potassium pump on the surface. In Eq. 7, the strength of sodium-potassium pump at surface depends on the ion's concentration, which leads

$$a^{Na} = 3\frac{I_p}{e}, \quad a^K = -2\frac{I_p}{e}, \quad a^{Cl} = 0, \quad (C.1)$$

where

$$I_p = I_{max1} \left(\frac{C_{in}^{Na}}{C_{in}^{Na} + K_{Na1}} \right)^3 \left(\frac{C_o^K}{C_o^K + K_{K1}} \right)^2 + I_{max2} \left(\frac{C_{in}^{Na}}{C_{in}^{Na} + K_{Na2}} \right)^3 \left(\frac{C_o^K}{C_o^K + K_{K2}} \right)^2. \quad (C.2)$$

We assume that the velocity at surface determines the characteristic velocity scale for the problem. We have ion fluxes in the intracellular, extracellular region in Eq. 5 and trans-membrane source of ion in Eq. 6 for ion Na^+, K^+, Cl^- .

At boundary of the intracellular space, due to the ion pump in Eq. C.1 and assumption of conductance at surface that $G^{Na} = G^{Cl} = 0$ [1, 3], we have

$$J_{in}^{Na} = a^{Na}, \quad J_{in}^K = j_s^K + a^K, \quad J_{in}^{Cl} = 0. \quad (C.3)$$

Since $g^K = 0$ inside of the lens, we obtain

$$j_s^K + a^K = 0. \quad (C.4)$$

This assumption obviously will have to be replaced in applications to other tissues, with a less particular distribution of channel proteins.

By the conservation of fluxes for each ion in Eq. 4, we get

$$J_{in}^i = -\delta_0 J_{ex}^i, \quad i = Na, K, Cl, \quad (C.5)$$

where $\delta_0 = \frac{M_{ex}}{M_{in}}$. Therefore, Eq. C.3 becomes

$$-\delta_0 J_{ex}^{Na} = a^{Na}, \quad -\delta_0 J_{ex}^K = 0, \quad -\delta_0 J_{ex}^{Cl} = 0. \quad (C.6)$$

Adding up all three fluxes in Eq. C.6 and since in the extracellular region each ion diffusion coefficient are at the same level of approximation, i.e.

$$D_{ex}^i = O(D_{ex}), \quad i = Na, K, Cl, \quad (C.7)$$

and based on Eq. 10, we get

$$O_{ex} u_{in} + \delta_0 D_{ex} \tau_c \frac{d}{dr} O_{ex} + \frac{D_{ex} \tau_c \delta_0}{k_B T} \rho_{ex} \frac{d}{dr} \phi_{ex} = a^{Na}. \quad (C.8)$$

The strength of the ion pump a^{Na} depends on the ion concentration in Eq. C.2. We choose the scale of a^{Na} is a^{Na*} based on an experimental estimation [1]. Using Eq. C.8, we take the scale for $O_{in,ex}$ and u_{in} to be O^* and u_{in}^* as

$$O^* = 2 \left(C_o^{Na} + C_o^K \right), \quad u_{in}^* = \frac{a^{Na*}}{O^*}. \quad (C.9)$$

By mass conservation expressed in Eq. 1, we naturally get the scale of u_{ex} as

$$u_{ex}^* = \delta_0^{-1} u_{in}^*. \quad (C.10)$$

Furthermore, $\phi^* = \frac{k_B T}{e}$ is used for the scale of electric potential ϕ_{in} and ϕ_{ex} . For the extracellular velocity in Eq. 2, we have

$$u_{ex}^* \tilde{u}_{ex} = -\frac{\kappa_{ex}}{\mu R} \tau_c P_{ex}^* \frac{d}{dr} \tilde{P}_{ex} - k_e \tau_c \frac{k_B T}{e R} \frac{d}{dr} \tilde{\phi}_{ex}, \quad (C.11)$$

We think the $\frac{d}{dr} P_{ex}$ term balance the velocity u_{ex} . The scale for extracellular pressure P_{ex}^* is then choose

$$P_{ex}^* = \frac{\mu R u_{ex}^*}{\kappa_{ex} \tau_c}.$$

Therefore, we get

$$\tilde{u}_{ex} = -\frac{d}{dr} \tilde{P}_{ex} - \delta_1 \frac{d}{dr} \tilde{\phi}_{ex}, \quad (C.12)$$

where $\delta_1 = \frac{k_e \tau_c k_B T}{e R u_{ex}^*}$. For the intracellular velocity, we have

$$u_{in}^* \tilde{u}_{in} = -\frac{\kappa_{in} P_{in}^*}{\mu R} \frac{d}{d\tilde{r}} \tilde{P}_{in} + \frac{\kappa_{in} \gamma_m k_B T O^*}{\mu R} \frac{d}{d\tilde{r}} \tilde{O}_{in}. \quad (\text{C.13})$$

We claim term $\frac{d}{d\tilde{r}} P_{in}$ and $\frac{d}{d\tilde{r}} O_{in}$ balance at the same level. Therefore, we choose the same scale for the intracellular and extracellular pressure, namely,

$$P^* = P_{in}^* = P_{ex}^*.$$

Then Eq. C.13 becomes

$$\delta_2 \tilde{u}_{in} = -\delta_3 \frac{d}{d\tilde{r}} \tilde{P}_{in} + \frac{d}{d\tilde{r}} \tilde{O}_{in}, \quad (\text{C.14})$$

where

$$\delta_2 = \frac{\mu R u_{in}^*}{\kappa_{in} \gamma_m k_B T O^*}, \quad \delta_3 = \frac{P^*}{\gamma_m k_B T O^*}.$$

In all, the fluid system Eq. 1 becomes

$$\begin{cases} \tilde{u}_{ex} = -\tilde{u}_{in}, \\ \delta_4 \frac{1}{\tilde{r}^2} \frac{d}{d\tilde{r}} (\tilde{r}^2 \tilde{u}_{in}) = \delta_3 (\tilde{P}_{ex} - \tilde{P}_{in}) + (\tilde{O}_{in} - \tilde{O}_{ex}), \end{cases} \quad (\text{C.15})$$

with boundary condition

$$\begin{cases} \tilde{P}_{ex} = 0, \\ \delta_5 \tilde{u}_{in} = \delta_3 \tilde{P}_{in} - (\tilde{O}_{in} - \tilde{O}_{ex}), \end{cases}$$

where

$$\delta_4 = \frac{\mathcal{M}_{in} u_{in}^*}{R \mathcal{M}_v L_m \gamma_m k_B T O^*}, \quad \delta_5 = \frac{u_{in}^*}{L_s \gamma_s k_B T O^*}.$$

Appendix C.2. Ions circulation

The velocity scales and diffusion coefficients in the extracellular and intracellular space are at different levels of approximation in our approach. In the following, we put the characteristic diffusion coefficients at intracellular and extracellular region and scale of concentration as

$$D_{ex}^* = D_{ex}^{Cl} \tau_c, \quad D_{in}^* = D_{in}^{Cl}, \quad C^* = C_o^{Na} + C_o^K.$$

In this way, we get Peclet number in the extracellular and intracellular and dimensionless Nernst potential as

$$Pe_{in} = \frac{u_{in}^* R}{D_{in}^*}, \quad Pe_{ex} = \frac{u_{ex}^* R}{D_{ex}^*}, \quad \tilde{E}^i = \frac{1}{z^i} \log \left(\frac{\tilde{C}_{ex}^i}{\tilde{C}_{in}^i} \right).$$

Because $g^{Na} = 0$ inside of lens, we have K^+ system as in Mathias's model [1],

$$\begin{cases} \frac{1}{\tilde{r}^2} \frac{d}{d\tilde{r}} \left(\tilde{r}^2 \left(Pe_{ex} \tilde{C}_{ex}^K \tilde{u}_{ex} - \tilde{D}_{ex}^K \left(\frac{d}{d\tilde{r}} \tilde{C}_{ex}^K + z^K \tilde{C}_{ex}^K \frac{d}{d\tilde{r}} \tilde{\phi}_{ex} \right) \right) \right) = 0, \\ \frac{1}{\tilde{r}^2} \frac{d}{d\tilde{r}} \left(\tilde{r}^2 \left(Pe_{in} \tilde{C}_{in}^K \tilde{u}_{in} - \tilde{D}_{in}^K \left(\frac{d}{d\tilde{r}} \tilde{C}_{in}^K + z^K \tilde{C}_{in}^K \frac{d}{d\tilde{r}} \tilde{\phi}_{in} \right) \right) \right) = 0, \end{cases} \quad (C.16)$$

with boundary condition

$$\begin{cases} \tilde{C}_{ex}^K = \tilde{C}_0^K, \\ Pe_{in} \tilde{C}_{in}^K \tilde{u}_{in} - \tilde{D}_{in}^K \left(\frac{d}{d\tilde{r}} \tilde{C}_{in}^K + z^K \tilde{C}_{in}^K \frac{d}{d\tilde{r}} \tilde{\phi}_{in} \right) = \frac{R_s}{z^K} (\tilde{\phi}_{in} - \tilde{E}^K) + \tilde{a}^K, \end{cases}$$

and Cl^- system as

$$\begin{cases} \frac{1}{\tilde{r}^2} \frac{d}{d\tilde{r}} \left(\tilde{r}^2 \left(Pe_{ex} \tilde{C}_{ex}^{Cl} \tilde{u}_{ex} - \tilde{D}_{ex}^{Cl} \left(\frac{d}{d\tilde{r}} \tilde{C}_{ex}^{Cl} + z^{Cl} \tilde{C}_{ex}^{Cl} \frac{d}{d\tilde{r}} \tilde{\phi}_{ex} \right) \right) \right) = \frac{\tilde{\mathcal{M}}_v^{ex}}{z^{Cl}} (\tilde{\phi}_{in} - \tilde{\phi}_{ex} - \tilde{E}^{Cl}), \\ \frac{1}{\tilde{r}^2} \frac{d}{d\tilde{r}} \left(\tilde{r}^2 \left(Pe_{in} \tilde{C}_{in}^{Cl} \tilde{u}_{in} - \tilde{D}_{in}^{Cl} \left(\frac{d}{d\tilde{r}} \tilde{C}_{in}^{Cl} + z^{Cl} \tilde{C}_{in}^{Cl} \frac{d}{d\tilde{r}} \tilde{\phi}_{in} \right) \right) \right) \\ = -\delta_8 \frac{1}{\tilde{r}^2} \frac{d}{d\tilde{r}} \left(\tilde{r}^2 \left(Pe_{ex} \tilde{C}_{ex}^{Cl} \tilde{u}_{ex} - \tilde{D}_{ex}^{Cl} \left(\frac{d}{d\tilde{r}} \tilde{C}_{ex}^{Cl} + z^{Cl} \tilde{C}_{ex}^{Cl} \frac{d}{d\tilde{r}} \tilde{\phi}_{ex} \right) \right) \right), \end{cases} \quad (C.17)$$

with boundary condition

$$\begin{cases} \tilde{C}_{ex}^{Cl} = \tilde{C}_0^{Na} + \tilde{C}_0^K + \delta_7 (\tilde{\phi}_{in} - \tilde{\phi}_{ex}), \\ Pe_{in} \tilde{C}_{in}^{Cl} \tilde{u}_{in} - \tilde{D}_{in}^{Cl} \left(\frac{d}{d\tilde{r}} \tilde{C}_{in}^{Cl} + z^{Cl} \tilde{C}_{in}^{Cl} \frac{d}{d\tilde{r}} \tilde{\phi}_{in} \right) = 0. \end{cases}$$

where

$$R_s = \frac{G^K k_B TR}{e^2 D_{in}^* C^*}, \quad \tilde{a}^K = \frac{a^K R}{D_{in}^* C^*}, \quad \tilde{\mathcal{M}}_v^{ex} = \frac{\mathcal{M}_v g^{Cl} k_B TR^2}{\mathcal{M}_{ex} e^2 D_{ex}^* C^*}, \quad \delta_8 = \frac{\mathcal{M}_{ex} D_{ex}^*}{\mathcal{M}_{in} D_{in}^*}.$$

The concentration of Na^+ can be solved from the following equations

$$\begin{cases} \sum_i z^i \tilde{C}_{in}^i + \tilde{z} \frac{\tilde{A}_{in}}{V_{in}} = \delta_6 (\tilde{\phi}_{in} - \tilde{\phi}_{ex}), \\ \sum_i z^i \tilde{C}_{ex}^i = -\delta_7 (\tilde{\phi}_{in} - \tilde{\phi}_{ex}), \end{cases} \quad (C.18)$$

where

$$\delta_6 = \frac{\mathcal{M}_v C_m k_B T}{e^2 C^* \eta}, \quad \delta_7 = \frac{\mathcal{M}_v C_m k_B T}{e^2 C^* (1 - \eta)}. \quad (\text{C.19})$$

From Eq. 11 and use the fact $z^{Na} = z^K = 1$ and assumption that $g^{Na} = g^{Cl}$ and $G^{Na} = G^{Cl} = 0$, we have

$$\begin{cases} \frac{1}{\tilde{r}^2} \frac{d}{d\tilde{r}} \left(\tilde{r}^2 \left(Pe_{ex} \tilde{\rho}_{ex} \tilde{u}_{ex} - \sum_i \tilde{D}_{ex}^i z^i \frac{d}{d\tilde{r}} \tilde{C}_{ex}^i - \tilde{\sigma}_{ex} \frac{d}{d\tilde{r}} \tilde{\phi}_{ex} \right) \right) = \tilde{\mathcal{M}}_v^{ex} \left(2 (\tilde{\phi}_{in} - \tilde{\phi}_{ex}) - \tilde{E}^{Na} - \tilde{E}^{Cl} \right), \\ \frac{1}{\tilde{r}^2} \frac{d}{d\tilde{r}} \left(\tilde{r}^2 \left(Pe_{in} \tilde{\rho}_{in} \tilde{u}_{in} - \sum_i \tilde{D}_{in}^i z^i \frac{d}{d\tilde{r}} \tilde{C}_{in}^i - \tilde{\sigma}_{in} \frac{d}{d\tilde{r}} \tilde{\phi}_{in} \right) \right) \\ = -\delta_8 \frac{1}{\tilde{r}^2} \frac{d}{d\tilde{r}} \left(\tilde{r}^2 \left(Pe_{ex} \tilde{\rho}_{ex} \tilde{u}_{ex} - \sum_i \tilde{D}_{ex}^i z^i \frac{d}{d\tilde{r}} \tilde{C}_{ex}^i - \tilde{\sigma}_{ex} \frac{d}{d\tilde{r}} \tilde{\phi}_{ex} \right) \right), \end{cases} \quad (\text{C.20})$$

with boundary condition

$$\begin{cases} \tilde{\phi}_{ex} = 0, \\ Pe_{in} \tilde{\rho}_{in} \tilde{u}_{in} - \sum_i \tilde{D}_{in}^i z^i \frac{d}{d\tilde{r}} \tilde{C}_{in}^i - \tilde{\sigma}_{in} \frac{d}{d\tilde{r}} \tilde{\phi}_{in} = \frac{R_s}{z^K} (\tilde{\phi}_{in} - \tilde{E}^K) + \tilde{I}_p^\phi, \end{cases} \quad (\text{C.21})$$

where

$$\tilde{\rho}_{in} = |z| \frac{\tilde{A}_{in}}{V_{in}} + \delta_6 (\tilde{\phi}_{in} - \tilde{\phi}_{ex}), \quad \tilde{\rho}_{ex} = \delta_7 (\tilde{\phi}_{ex} - \tilde{\phi}_{in}), \quad \tilde{I}_p^\phi = \frac{I_p R}{e D_{in}^* C^*},$$

and

$$\tilde{\sigma}_{in} = \sum_i \tilde{D}_{in}^i (z^i)^2 \tilde{C}_{in}^i, \quad \tilde{\sigma}_{ex} = \sum_i \tilde{D}_{ex}^i (z^i)^2 \tilde{C}_{ex}^i.$$

Appendix D. Effect of permeability

- [1] R. T. Mathias, *Steady-state voltages, ion fluxes, and volume regulation in syncytial tissues* 48 (3) (1985) 435–448.
URL <http://linkinghub.elsevier.com/retrieve/pii/S0006349585837991>
- [2] D. T. K. Malcolm, *A computational model of the ocular lens*, Ph.D. thesis, ResearchSpace@ Auckland (2006).
- [3] J. Gao, X. Sun, L. C. Moore, P. R. Brink, T. W. White, R. T. Mathias, *The effect of size and species on lens intracellular hydrostatic pressure*, *Invest Ophthalmol Vis Sci* 54 (1) (2013) 183–92. doi:10.1167/iops.12-10217.
URL <http://www.ncbi.nlm.nih.gov/pubmed/23211824>

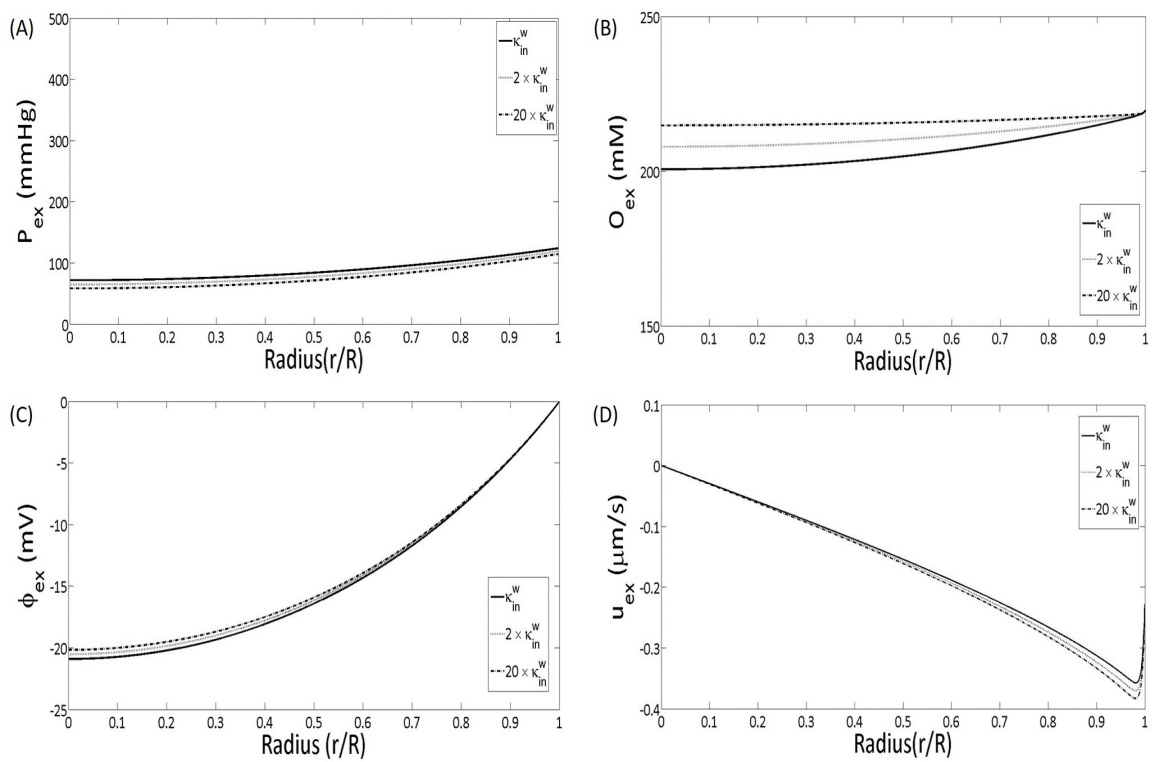


Figure D.1: Comparison between different κ_{in} .